CHALMERS
UNIVERSITY OF TECHNOLOGY

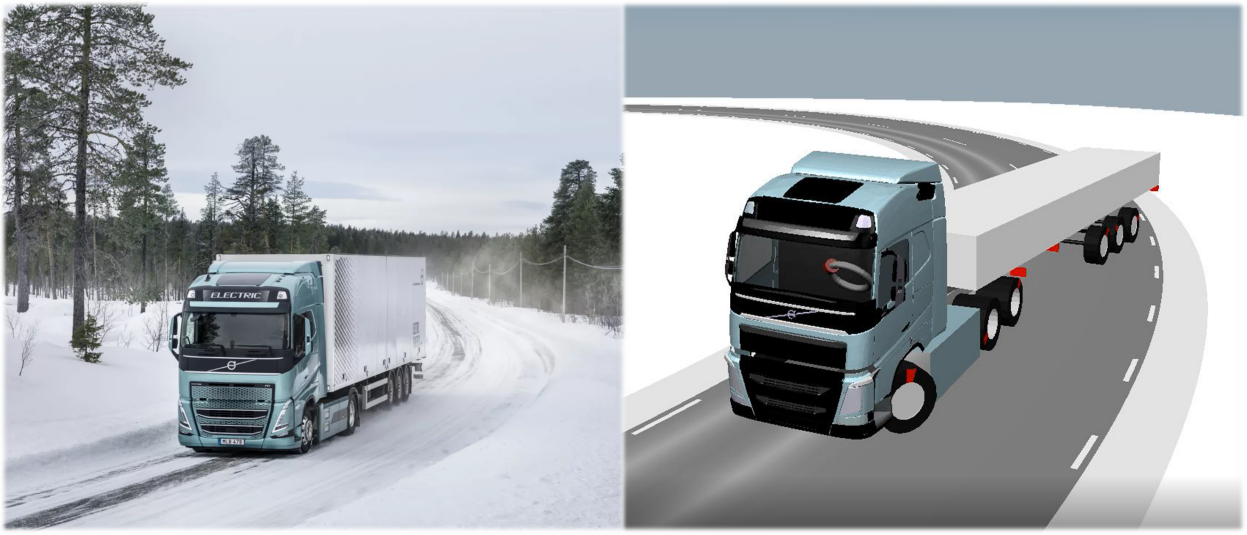

Safe operating envelope for electric semi-trailer

On safe driving conditions with electric trailer propulsion for heavy truck combinations using coordinated vehicle motion control

Master's thesis in Systems Control and Mechatronics

Erik Andersson
Axel Hansson

DEPARTMENT OF MECHANICS AND MARITIME SCIENCES
CHALMERS UNIVERSITY OF TECHNOLOGY
Gothenburg, Sweden 2022
www.chalmers.se

Master's thesis in systems, control and mechatronics

Safe operating envelope for electric semi-trailer

On safe driving conditions with electric trailer propulsion for heavy truck combinations using coordinated vehicle motion control

ERIK ANDERSSON
AXEL HANSSON

CHALMERS
UNIVERSITY OF TECHNOLOGY

Department of Mechanics and Maritime Sciences
Division of Vehicle Engineering and Autonomous Systems
Chalmers University of Technology
Gothenburg, Sweden 2022

Safe operating envelope for electric semi-trailer
On safe driving conditions with electric trailer propulsion for heavy truck combinations using coordinated vehicle motion control
ERIK ANDERSSON
AXEL HANSSON

Supervisors:
Leo Laine, Volvo Group Trucks Technology
Maliheh Sadeghi Kati, Volvo Group Trucks Technology
Umur Erdinç, Volvo Group Trucks Technology

Examiner:
Mats Jonasson, Mechanics and Maritime Sciences, Chalmers

Master's Thesis 2022:26
Department of Mechanics and Maritime Sciences
Division of Vehicle Engineering and Autonomous Systems
Chalmers University of Technology
SE-412 96 Gothenburg
Telephone +46 31 772 1000

Cover: Real electric tractor semi-trailer vehicle combination (left) and simulated vehicle in similar conditions exhibiting trailer swing (right).

Typeset in LaTeX
Printed by Chalmers Reproservice
Gothenburg, Sweden 2022

Safe operating envelope for electric semi-trailer
On safe driving conditions with electric trailer propulsion for heavy truck combinations using coordinated vehicle motion control
ERIK ANDERSSON
AXEL HANSSON
Department of Mechanics and Maritime Sciences
Chalmers University of Technology

Abstract

With higher demands on electrification of the transport sector comes new challenges regarding the range of battery electric heavy vehicles. Installing batteries in the trailers of a heavy vehicle combination allows for an increase in range and also gives the opportunity of adding electric motors to the trailer. However using an electric trailer for propulsion may introduce stability issues which, if found, must be accounted for and controlled in order to not decrease the performance of the electric vehicle compared to the conventional tractor semi-trailer vehicles.

This thesis presents an investigation on when and how an electric trailer can be used for propulsion and coordination of a heavy tractor semi-trailer vehicle combination. Definitions of what is regarded as safe motion of the vehicle is defined and a limiting operating envelope for the electric trailer is developed using data attained from simulations. Control systems which include control allocation are developed to coordinate the two vehicle units and to distribute forces among each of the available motion and steering actuators on the vehicle. The systems are verified and tested in a high fidelity simulation environment for two test cases, the first of which is to travel through an S-curve consisting of two opposing 90° turns and the second is the standardized "Sine with dwell" test (ISO 18375:2016).

The proposed control systems perform well for the two presented test cases with some limitations regarding the scenario parameters. Additional predictive control systems are proposed as a possible improvement to the current systems. In the thesis, electric trailers are proven to, in concept, be a viable way of propelling, braking and controlling a two-unit vehicle combination using a safe operating envelope and control allocators.

Keywords: Heavy trucks, control theory, control allocation, vehicle safety, semi-trailer, electric vehicle, operating envelope, actuator coordination, simulation.

Acknowledgements

Firstly we would like to thank and express our gratitude to our supervisors at Volvo GTT, adjunct professor Leo Laine, postdoctoral researcher Maliheh Sadeghi Kati and industrial doctoral student Umur Erdinç for their continuous support and incredibly helpful and inspiring discussions we have had with you during our thesis. Your time spent assisting us during our work has been invaluable.

We would like to thank our examiner Mats Jonasson at Chalmers University of Technology for his support and constructive feedback on our work and encouragement throughout our thesis.

We would also like to thank Volvo GTT and all employees at the VMM team for presenting us with the opportunity of writing this thesis. Thank you to Chalmers Centre for Computational Science and Engineering, C3SE, for allowing us to use their computer cluster. Lastly we would like to thank the other thesis workers we have met during our thesis for the interesting discussions we have had and, of course, their great company.

Erik Andersson, Gothenburg, June 2022
Axel Hansson, Gothenburg, June 2022

List of Acronyms

Below is the list of acronyms that have been used throughout this thesis listed in alphabetical order:

BEV	Battery electric vehicle
CoG	Center of gravity
E-trailer	Electric trailer
EM	Electric motor
GTT	Group Trucks Technology
ICE	Internal combustion engine
NTP	Normal temperature and pressure
SB	Service brake
SLS	Sequential least squares
SoC	State of charge
SOE	Safe operating envelope
VTM	Volvo Transport Model
WLS	Weighted least squares
YSF	Yaw stability factor

Nomenclature

Below is the nomenclature of indices, parameters, and variables that have been used throughout this thesis.

Indices

i	Index for vehicle unit
j	Index for axle on vehicle unit
s	Index for side of axle on vehicle unit (L or R)

Note: Indexing unit number, axle number and side of axle is done for all variables in the order ijs, i.e. for electric motor torque: $T_{ijs,em}$

tot	Abbreviation for total, sum of all parameters/variables with the same name.
V	Index for total force/moment in vehicle frame (excluding external forces)
c	Combination level
em	Electric motor
sb	Service brake
res	Resistance
req	Request
ref	Reference
e	Variable included in SOE
P	Power limited
μ	Friction limited

Parameters

γ	Penalty coefficient
n	Number of vehicle units
a_i	Number of wheel axles
R_r	Radius of turn in road
μ	Road-tire friction coefficient
T	Applied torque on each driven wheel on trailer
g	Gravitational acceleration (9.81 $\frac{m}{s^2}$)
r_{ijs}	Wheel radii
m_{ij}	Axle loads
$\boldsymbol{u}$	Input signals
$\boldsymbol{v}$	Virtual control signals
B	Control efficiency matrix
$\boldsymbol{u}_{des}$	Desired input signals
W_u	Input signal weight matrix
W_v	Virtual control signal weight matrix
C_{ij}	Tire cornering stiffness factor
$l_{a,ij}$	Longitudinal position of axle relative CoG of unit
w_{ij}	Track width
J_i	Moment of inertia
P_{em}	Power output of electric motor
c_d	Air drag coefficient
A	Frontal area of tractor
ρ	Air density
δ_u	Allowed control range of δ_{11}
η	Brake ratio
ζ	Safety ratio for friction limit
d_{r_1}	Distance from CoG of first unit to its rear coupling point
d_{f_2}	Distance from CoG of second unit to its front coupling point
$\boldsymbol{\lambda}$	Longitudinal force distribution vector
$\boldsymbol{\kappa}$	Brake force distribution vector

Variables

$F_{x,i}$	Sum of all longitudinal forces acting on unit
$F_{y,i}$	Sum of all lateral forces acting on unit
$F_{cxr,i}$,$F_{cyr,i}$	Rear coupling forces in x- and y-direction
$M_{z,i}$	Sum of all moments about the z-axis
$a_{x,i}$	Total longitudinal acceleration
$a_{y,i}$	Total lateral acceleration
α_{ij}	Lateral slip of axle
θ_i	Articulation angle between unit i and $i+1$
δ_{ij}	Steering angle
ω_w	Rotational speed of wheel
$F_{roll,ijs}$	Rolling resisting force
F_d	Air drag force
$M_{y,ijs}$	Rolling resistance torque from wheel

Contents

List of Figures

List of Tables

1

Introduction

1.1 Background

The total global carbon emissions footprint made by humans have for the past decades increased exponentially and are expected to keep increasing in the years to come. In 2020, the road transport sector which include heavy-duty trucks used in for instance construction, logging and refrigeration, are estimated to have accounted for 5% of the total global CO2 emissions and 30% of the global CO2 emissions in the transport sector [1], [2]. Research of battery electric vehicles (BEVs) is a popular topic in the heavy vehicle industry as it serves as an environmentally sustainable alternative to combustion engines run with fossil fuels. Several companies in the heavy truck industry aim at in the future only to sell and produce trucks which only use electrical power as the main source of propulsion [3].

One of the many issues with battery operated heavy trucks is to maintain an equivalently long range as their fossil fuel powered counterparts. Volvo Trucks currently offers several of its models with electric powertrains. Out of these models, the Volvo FM Electric, is able to achieve a range of up to 380 km [4], which is the longest ranging Volvo BEV truck. This is an adequate range for short haul transportation in urban areas like cities and industrial areas. However, for long haul transportation a truck driver in the European Union is allowed to drive for a maximum of 10 hours per day [5], which at 90 km/h results in a distance of up to 900 km per day. Using Volvo's existing electric trucks for long haul transportation thus becomes inconvenient since two time consuming recharges are required.

A novel solution to extend the range of a vehicle is to add more batteries, thus increasing the total energy capacity on board. If batteries and electrical motors are installed in the trailer of a tractor semi-trailer combination, the trailer could be used as a propulsive complement to the vehicle. This allows for the possibility of using an electric trailer (e-trailer) on both tractors with internal combustion engines (ICEs) and on BEV-tractors. The e-trailer could also be used to recharge the batteries through regenerative braking, thus preventing wasting energy through the mechanical braking system.

Conventional heavy truck trailers are normally installed with pneumatic brakes to make the vehicle stop safely and in time. To achieve the maximum possible range of a BEV, it could be necessary to deplete the batteries in order to allocate more

capacity when using regenerative braking. This would require extensive knowledge on whether safe driving can be ensured or not when the trailer is accelerating or retarding the vehicle combination. Safe driving is throughout the thesis defined as when the vehicle is not in any of the unsafe modes depicted in Figure 1.1. By investigating and controlling the acceleration and braking requests from the truck driver when driving with an e-trailer in different conditions and scenarios, safe driving can be ensured without running the risk of putting the driver or truck in a dangerous situation. A set of requested forces and moments (from the physical driver or autonomous system) together with additional parameters such as road profile and longitudinal speed of the vehicle which ensures safe driving is called a safe operating envelope (SOE). This envelope can therefore determine what user inputs will yield safe vehicle motion and which will not.

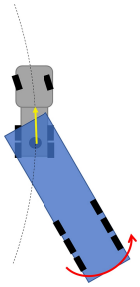

(a) Wheels on trailer slip while tractor does not slip, causing trailer swing

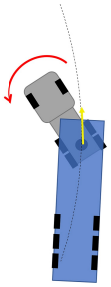

(b) Wheels on tractor's two rear axles slip while trailer does not slip, causing a jack-knife

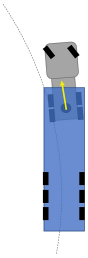

(c) Wheels on tractor's front axle slip while the rest of the vehicle does not slip, causing off-tracking due to understeering

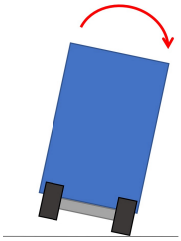

(d) The trailer rolls over on to its side, causing a roll-over

Figure 1.1: Unsafe modes of tractor (grey) and semi-trailer (blue) in combination. Red arrows indicates tractor or trailer motion and yellow arrows indicates the coupling point's direction of travel

1.2 Purpose

The purpose of this thesis is to investigate whether it is possible to, in a safe manner, use an e-trailer for propulsion in a vehicle combination. The work will be focused around using a two unit vehicle combination where both units can be used as propulsion units. This enables for unconventional propulsion strategies to be used, instead of the more traditional setup where only the tractor is pulling the vehicle. For example the vehicle combination may be propelled by only using the batteries and

electric motors of the e-trailer while the first unit is used for braking only. The ultimate motivation of using an e-trailer for propulsion is to increase the range of BEV trucks. Also, the suggested propulsion strategies are to be constructed such that unsafe vehicle behavior, as described in section 1.1, can be avoided during normal driving conditions.

1.3 Objective

In order to fulfill the purpose of the thesis a set of objectives are set up:

- Define proper and realistic conditions for safe driving without putting the vehicle and driver in a dangerous situation, such as critical thresholds for jackknifing and trailer swing.
- Find a safe operating envelope which enclose conditions for safe driving. With provided inputs, the SOE determines whether the safe driving of the vehicle is ensured or not and if the inputs from the driver must be limited or not.
- Develop a control allocator for combinations of units that can distribute the total forces acting on the entire vehicle between the individual units.
- Develop control allocators and necessary control algorithms to be used within each individual unit, using distributed forces as inputs.
- A method and function for optimizing the power use on the vehicle by controlling electrical and mechanical brakes will be developed in order to minimize the amount of energy wasted on conventional service brakes.

1.4 Scope

The scope of the thesis is limited to:

- Studying one specific vehicle combination, shown in Figure 1.2. The vehicle is a 6x4 BEV-tractor (three axles in total, axle two and three being driven) combined with a 6x4 electric semi-trailer (three axles in total, axle one and two being driven).
- Defining a SOE for a limited number of predefined test cases for the vehicle combination such that satisfactory results and conclusions can be drawn within the time limitations of the thesis. The test cases will for instance only include flat roads with no incline, decline or camber.
- The SOE is limited to only consider longitudinal velocity of the first unit, articulation angle between the units, road surface friction coefficient, requested torque on trailer and longitudinal and lateral coupling forces.
- Available actuators on the vehicle include:
  - electric motors on each wheel on axles 2 and 3 of the tractor and each wheel on axles 1 and 2 of the trailer

  - mechanical service brakes on all wheels of the vehicle
  - steering of the wheels on axle 1 of the tractor
- Energy usage of vehicle is not studied. However, efforts to minimize energy usage on the vehicle regarding actuator usage will be done but without quantifying actual energy effectiveness.

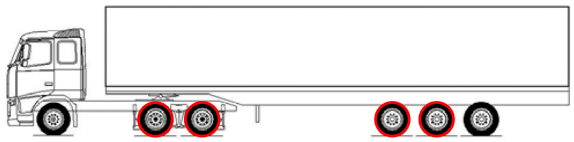

Figure 1.2: 6x4 tractor combined with a 6x4 electric semi-trailer. Driven axles are marked in red.

1.5 Limitations

Limitations of the thesis and topics not studied include:

- Detailed analysis of energy usage on the vehicle.
- Battery modeling and charge cycles of batteries.
- Development and verification of proposed control system is carried out solely through simulations since no physical e-trailer is available

1.6 Ethical aspects

The objective and scope of the thesis is to develop a driver assist and control system, which can be regarded as a semi-autonomous system. The driver will be assisted in controlling the motion of the vehicle in more ways than the driver ever could do on their own. Therefore the driver will rely on that the system responds in the correct way to the driver's inputs. If the driver is confident in the system and devotes trust in the robustness and functionality of it, then the driver might lose essential skills maneuvering the vehicle which is needed if the system fails or is not active. It could also lead to driver inattentiveness and negligence of the current road conditions which, since the system is neither autonomous nor self-driving, could lead to dangerous driving situations as discussed in [6]. Further discussed in [6] is the responsibility of safety systems in automated vehicles. It is from the article evident that a vehicle with advanced safety systems will to a certain extent carry the responsibility of any possible accident caused by for instance malfunctioning software, as opposed to a vehicle without such systems in which the driver would be carrying almost all responsibility. Software bugs, misbehaving safety functions, issues regarding hacker attacks due to wanting cyber security and incorrect use of the safety functions can all risk causing large costs in terms of human suffering and material and financial damage.

A successful implementation of a control and safety system which minimizes energy usage in electric heavy trucks can benefit the transition from using fossil fuels to renewable energy sources in the transport sector. The 17 Sustainable Development Goals presented by the United Nations [7] aims for peace and prosperity for the entire planet, for instance through slowing down climate change and ensuring good health and well-being for all people. This thesis present ways to for instance help reduce the use of fossil fuels and consequently decreasing the number of people affected by air pollution related illnesses. The transition in the transport sector to renewable energy sources can also help create sustainable cities and communities and promote sustained economic growth.

The extensive use of model based design and simulations when developing the functions and systems in the thesis eliminates the need for real life tests to a large extent. This avoids using fossil fuels in vehicles, fatigue and stress on the vehicle and road and thus avoids unnecessary carbon emissions and pollution. Also, damage caused to the physical vehicle, its surroundings and the driver may be reduced by first verifying that the developed systems functions as intended through simulations.

1.7 Disposition

The model of the studied vehicle combination is presented in chapter 2 followed by a definition and description of the safe operating envelope in chapter 3. The complete control system used to control the vehicle with the SOE implemented is presented in chapter 4 followed by results from comparing the obtained control system with some reference systems in chapter 5. The results are discussed and conclusions about the work in the thesis are drawn in chapter 6 together with recommendations for future work. Appended are mathematical derivations in Appendix A, chosen vehicle specifications in Appendix B and test results in Appendix C.

2

Vehicle modeling

In order to apply model based design in the development process of the thesis, consistent definitions of metrics and high fidelity models of the vehicle and its subsystems are needed. This chapter provides material of how the vehicle models are set up and will be the basis of what methods are used later on in the thesis.

2.1 Volvo Transport Model

Volvo Group Trucks Technology (GTT) has developed non-linear high fidelity mathematical models of the tractor semi-trailer combination, which are used for simulating the vehicle during function development. The library is referred to as Volvo Transport Model (VTM), and is built in MATLAB/Simulink. It includes complete models of different vehicle combinations and provides functionality to create different customized combinations using available base models. These models include for instance tire, cab, steering and chassis models.

VTM is built up using rigid bodies for the cab and the wheel axles and two rigid bodies for the frame which can warp to account for continuous frame torsion [8]. The bodies are individually suspended to neighbor bodies and can all move in 6 degrees of freedom with regards to a set stiffness and damping factors.

This model has been, for a number of vehicle combinations, tested and verified to be accurate enough for control system development through comparison with real life tests [9], [10]. The Magic Tire Formula [11] is used as the tire model in VTM for all vehicle combinations.

Figure 2.1 shows a simplified example of the VTM block in Simulink. The VTM block computes the vehicle combination's motion and positions, and requires steering angles and wheel torques as well as drag force.

VTM provides comprehensive sensor data from the simulated vehicle. Data buses are used to obtain data from each individual component. Since the model is purely mathematical it is possible to obtain accurate simulated measurements from components that is not normally fitted with sensors or difficult to measure in real life. This is beneficial when developing new functions since many of the commonly used sensor data signals is readily available in many different locations on the vehicle. For example there are data buses available for each individual tire, wheel axle, front and rear of each unit as well as the cab. The information transmitted in the data

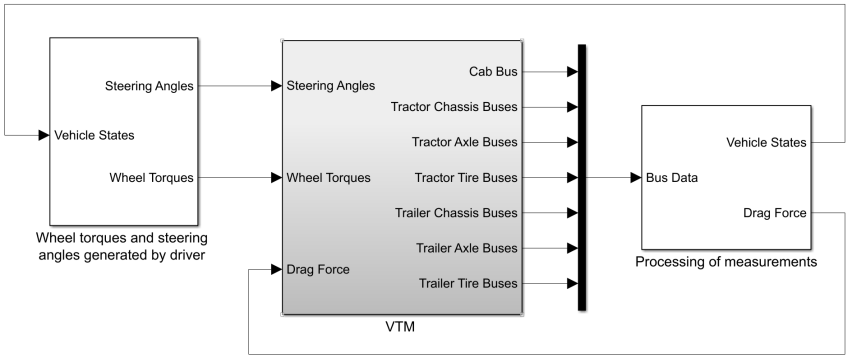

Figure 2.1: Conceptual Simulink plant using a simplified VTM block

buses differs depending on the component but can include for example local and global positions and velocities of the components as well as their angular velocities. The tire buses includes longitudinal and lateral slip, applied forces and moments.

Electric motors, speed controllers, external resistance models and path following controllers are not included in the VTM library and will thus be defined thoroughly in this chapter. The VTM model and its subsystems will not be described in further detail since it is Volvo GTT's internal model used for function development.

2.2 Coordinate frames and model definitions

In order to describe motion and dynamics of the different vehicle units a definition of coordinate systems and global forces acting on them is required. For this the international standard for road vehicles ISO 8855 [12] is used, see Figure 2.2.

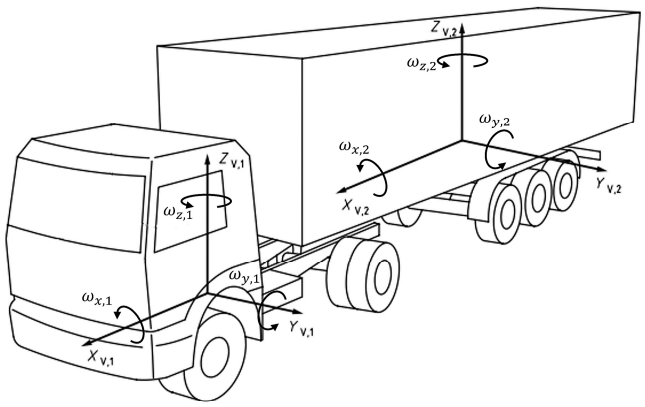

Figure 2.2: Vehicle coordinate frame for a tractor with a connected semi-trailer

$X_{V,i}$,$Y_{V,i}$,$Z_{V,i}$ are the unit axis systems where $i \in \{1, 2, \ldots n\}$ with the leading unit getting unit number 1 and trailing units getting increasingly higher numbers. n is the total number of units of the vehicle, which in any studied vehicle combination

may include tractors, trucks, trailers and dollies. Forces, angles, moments and dimensions are defined per unit on the studied vehicle. A general description of this is depicted in Figure 2.3 where unit i is related to a leading and a trailing unit. If unit i is the first unit of the vehicle, then coupling point $i-1$ is disregarded together with all associated dimensions. If unit i is the last unit of the vehicle, then coupling point $i+1$ is disregarded together with all associated dimensions. The coupling points of consecutive units (purple points) are separated for clarity. However in the model and in reality they coincide with each other.

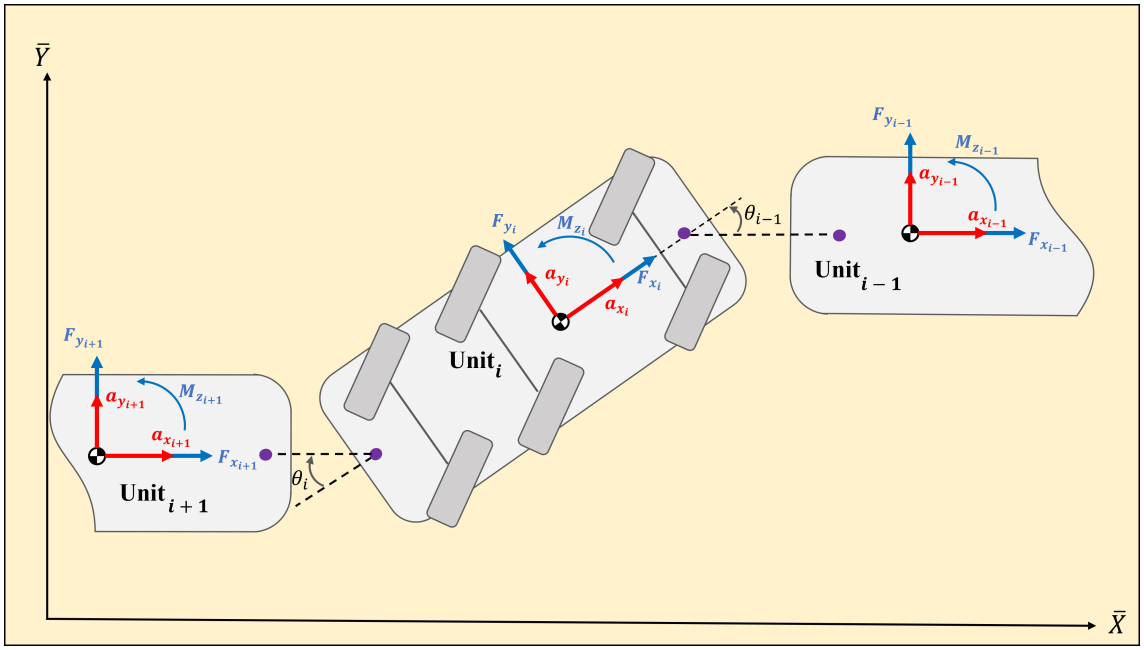

Figure 2.3: Definition of total forces acting on each unit of vehicle combination

Local forces $F_{x,i}$ and $F_{y,i}$ denotes the unit's total longitudinal and lateral forces respectively, with the origin in its center of gravity (CoG). Similarly, accelerations and moments on each unit are defined in the same coordinate frame as the local forces on each unit. The world frame in which the vehicle moves in are denoted by the coordinates $\bar{X}$, $\bar{Y}$, $\bar{Z}$.

The total forces in Figure 2.3 can be deconstructed into all forces acting on each unit, which include forces acting on each wheel, coupling forces and resulting forces from air resistance and rolling resistance. This is shown in Figure 2.4. The index 'V' denotes forces on the unit, excluding external forces such as coupling forces and resulting forces. The forces $F_{x_{V,i}}$, $F_{y_{V,i}}$ and $M_{z_{V,i}}$ is only used to represent and gather all forces shown in blue in Figure 2.4. The longitudinal forces are split into forces resulting from the electric motors ,'em', $F_{x_{V,i,em}}$ and from the service brakes ,'sb', $F_{x_{V,i,sb}}$. There are coordinate frames for each coupling point for each unit to translate forces between units properly.

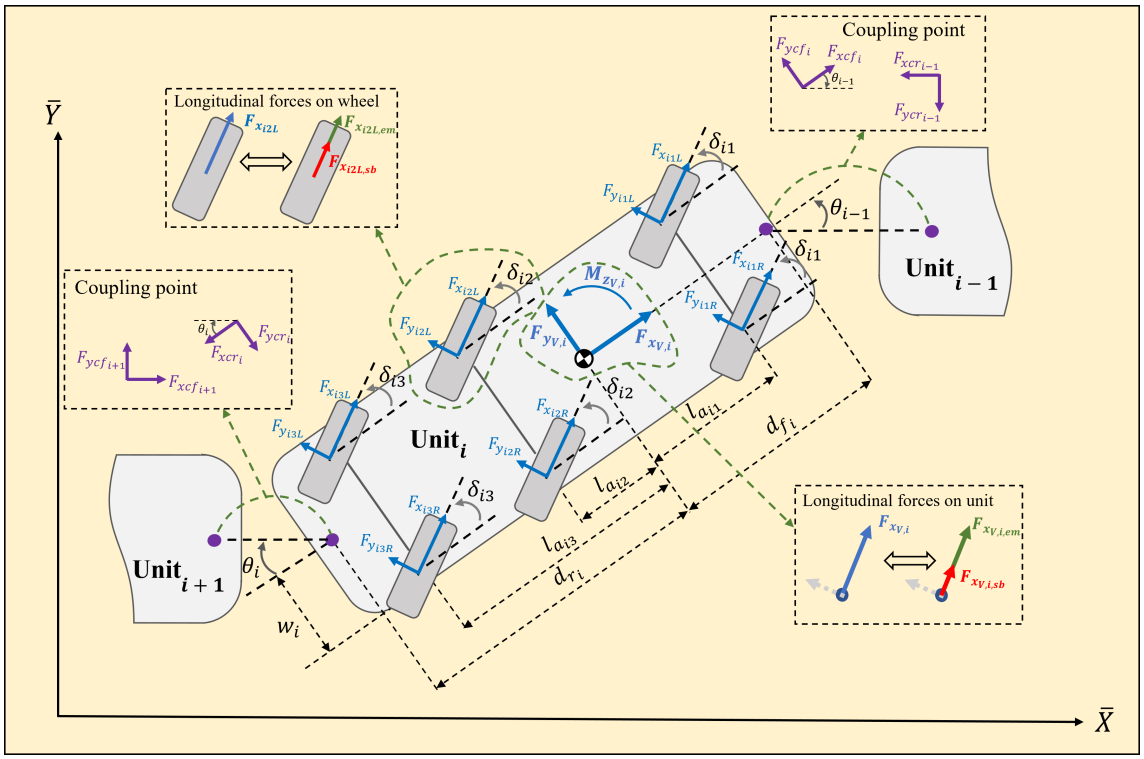

Figure 2.4: Definitions of metrics for vehicle unit i with 3 axles and its relations to leading and trailing units

2.3 Electric motors

All electric motors are modeled as low pass filters which filters the requested torques of each motor. The low pass filter is used to model the response time of the electric motors, which will appear as a time delay during simulations. Each wheel that is connected to an electric motor will then be subjected to the requested torque but with a slight time delay. The electric motors are torque- and power-limited which is presented in Equations 4.25-4.28.

The low pass filter in Equation 2.1 adds a delay on the requested torque with a time constant of 0.3 seconds, and this is the transfer function used to model the electric motors of both the tractor and trailer.

$$G_{LP,em}(s) = \frac{1}{0.3s + 1} \tag{2.1}$$

Similarly, the transfer function for the time delay for the mechanical service brakes is set as a slightly longer delay:

$$G_{LP,sb}(s) = \frac{1}{0.5s + 1} \tag{2.2}$$

During the construction of the safe operating envelope in chapter 3, the motors are lumped together per axle on all units such that both wheels on each axle are given the same torque when accelerating or decelerating. The motors are however not

lumped together during all other parts of the thesis. It is also assumed that the power output from each motor is directly proportional to the speed of the motors.

2.4 Driver Model

Since the vehicle is simulated there is no physical driver controlling the vehicle's velocity or heading. Thus, a mathematical driver model is needed in order to control the vehicle. The driver model consist of two subsystems, a speed controller and a path follower.

2.4.1 Speed controller

During the simulation process a speed controller will be used to control propulsion. The controller will enable the vehicle to accelerate, decelerate and maintain requested velocity automatically throughout the simulations.

The speed controller used is a PID controller, described in Equation 2.3. Because the controller will be used to maintain a requested velocity, it will act on the error between the requested velocity and the current velocity of the vehicle. That is, $e = v_{x,req} - v_x$.

$$F_{x,req} = e\left(K_p + K_i\frac{1}{s} + K_d\frac{K_n}{1 + K_n\frac{1}{s}}\right), \tag{2.3}$$

where $K_p = 5 \cdot 10^5$, $K_i = 1 \cdot 10^3$, $K_d = 7 \cdot 10^3$ and $K_n = 100$.

The speed controller computes the total requested propulsion force that is needed in order to reach requested velocity. Since not all axles are driven, the force is proportionally distributed between the driven axles. Each axle is allotted force proportional to the axle load in relation to the total axle load of the driven axles of that unit. Finally, the speed controller outputs both requested wheel torques and the total requested acceleration. Wheel torques are obtained by multiplying the requested forces with the corresponding wheel radii and acceleration is obtained by dividing the total force by the total mass of the vehicle. Depending on the application in the simulations, both torques and acceleration can be useful.

Some system limitations are also considered in the speed controller modeling. Firstly, the total propulsion force that the controller outputs cannot exceed the total force that the electric motors can produce. Secondly, the force distributed to each wheel cannot exceed the maximum friction force available. This limitation is implemented in order to prevent the vehicle from losing traction.

2.4.2 Path follower

A steering controller that adjusts the vehicle's steering angle to follow the desired path is needed. This is handled by a PID controller acting on the lateral distance error between the center of the front most axle and the desired path.

In order to obtain the distance between the center of the axle and the desired path, the velocities of the axle specified in the world coordinate frame are used. These velocities are then expressed as velocities in the coordinate frame of the path, where ξ expresses the longitudinal distance traveled and ν expresses the lateral displacement from the path. The change of coordinate frame from the world frame to that of the road is done by using the rotation matrix

$$\begin{bmatrix} v_\xi \\ v_\nu \end{bmatrix} = \begin{bmatrix} \cos(\varepsilon) & -\sin(\varepsilon) \\ \sin(\varepsilon) & \cos(\varepsilon) \end{bmatrix} \begin{bmatrix} v_{\overline{X}} \\ v_{\overline{Y}} \end{bmatrix}, \tag{2.4}$$

where $v_{\overline{X}}$, $v_{\overline{Y}}$ are velocities in the world frame and v_ξ, v_ν are the corresponding velocities in the coordinate frame of the path. The rotation angle or the vehicle heading specified in the world coordinate frame, ε, is computed by integrating the angular velocity of the path, $\omega_{z,path}$

$$\varepsilon = \int \omega_{z,path}\, dt = \int v_\xi C(x_\xi)\, dt \tag{2.5}$$

where $C(x_\xi)$ is the curvature of the path as a function of the traveled length of the path, x_ξ. The obtained lateral velocity in the coordinate frame of the path, ν, describe at what velocity the front axle of the vehicle deviates from the path. Integrating the lateral velocity gives the lateral distance between the center of the axle and the path, ν, which is the input to the PID controller. The controller outputs the requested steering angle, $\delta_{11,req}$, according to

$$\delta_{11,req} = x_\nu \left(K_p + K_i \frac{1}{s} + K_d \frac{K_n}{1 + K_n \frac{1}{s}} \right), \tag{2.6}$$

where $K_p = -1$, $K_i = -1 \cdot 10^3$, $K_d = -0.1$ and $K_n = 100$.

2.4.3 Motion resistance forces

Forces on the vehicle from longitudinal air resistance is calculated as

$$F_d = c_d \frac{1}{2} \rho v_x^2 A \tag{2.7}$$

where c_d is estimated to be 1, $A = 5.2$ is set as the frontal area of the tractor and $\rho = 1.204$ is set after the normal temperature and pressure (NTP) of air. The rolling resistance is estimated from the rolling resistance torques obtained from the tire model $M_{y,ijs}$ where i denotes the vehicle unit, j denotes the axle on the unit and s denoted the side of the axle (left or right). Together with the radii of the tires on the vehicle each rolling resistance force is related as

$$F_{roll,ijs} = \frac{M_{y,ijs}}{r_{ij}} \tag{2.8}$$

$$F_{roll,i} = \sum_{j=1}^{a_i} \sum_{s=[l,r]} F_{roll,ijs} \tag{2.9}$$

$$F_{roll,tot} = \sum_{i=1}^{n} F_{roll,i} \tag{2.10}$$

where n is the number of units and a_i is the number of axles on unit i. The total resistance forces for each unit thus becomes:

$$F_{res,1} = F_d + F_{roll,1} \tag{2.11}$$

$$F_{res,i} = F_{roll,i}, \quad \text{for } 1 < i \leq n \tag{2.12}$$

3

Safe Operating Envelope

A set of applied actuator signals together with environmental parameters and vehicle states which, by some logic, can predict or ensure safe driving with a high probability is called a safe operating envelope. Safe operating envelopes are used in the flight industry and have been well studied [13], [14]. The use of SOEs as a limiting function regarding the capabilities of heavy vehicles and ensuring safe driving has been studied and researched using model predictive controllers on yaw rate and wheel side slip angle [15]–[17]. It has however not been done using off-line generated simulated experimental data with different and more versatile envelope parameters to limit an e-trailer in a two-unit heavy vehicle combination. Such off-line computing will thus be studied in this thesis. By using experimental data in the envelope it is independent of the internal dynamics of the vehicle and is instead based on simulated measurements.

3.1 Defining safe vehicle motion

In order to classify the movement of the simulated vehicle combination proper definitions of what is considered safe are set up. This is done by first listing the unsafe behaviors. These can be summarized into the four possible scenarios depicted in Figure 1.1, repeated here for convenience:

- Off-tracking due to understeering
- Jack-knife of vehicle combination due to tractor wheels slipping
- Trailer swing due to trailer wheels slipping
- Vehicle rollover

Unsafe behavior due to off-tracking, as depicted in Figure 1.1c, is considered to occur when the lateral displacement of the center of the front most axle of the leading unit is more than half the width of a single lane from the center of the lane. Highway lanes close to rural areas in Sweden are required to be at least 3.25 meters wide [18]. The threshold for off-tracking is therefore set to 1.75 m.

A jack-knife situation is detected by using the lateral slip of both the tractor and the trailer together with the articulation angle between the units. The definition of jack-knife, as in Figure 1.1b, specifies that the rear axles of the tractor should lose traction while the axles of the trailer should maintain traction. The lateral slip of

the tractor's rear axles will thus be high and the lateral slip of the semi-trailer will be low. Based on experience from simulations the thresholds for lateral slip, α, are chosen as

$$\alpha_{12} = \frac{|v_{y,12}|}{|v_{x,12}|} > 0.8 \tag{3.1}$$

$$\alpha_{22} = \frac{|v_{y,22}|}{|v_{x,22}|} < 0.4, \tag{3.2}$$

where index 12 and 22 represents the second wheel axle of the first and second unit correspondingly. The threshold values are chosen from experience in simulations. Also, in order to further define jack-knifing, a lower limit on the articulation angle, θ, is added. Since jack-knifing only poses a danger for the vehicle when the tractor and trailer crashes into each other, $|\theta| \geq 90°$ is used as an additional condition which defines jack-knifing. When all three thresholds are fulfilled, jack-knifing is considered to occur.

The definition used for trailer swing is similar to the one of jackknifing. The main difference is that the tractor maintains traction and the trailer does not. Therefore the thresholds for lateral slip are reversed; $\alpha_{12} > 0.4$ and $\alpha_{22} < 0.8$. The threshold for articulation angle between the units is set to $|\theta| \geq 30°$.

The last unsafe behavior, vehicle rollover, includes scenarios when the vehicle rolled over to its side. The threshold used is simply a roll angle of 90° for the tractor or trailer.

Scenarios not included in the unsafe behaviors are considered to be safe. The first safe scenario is when the simulated vehicle manages to travel all the way through a simulated test track. There is also the possibility that the vehicle brakes to a complete stop, without fully completing the track. Both these scenarios are deemed safe since neither suffers from any of the unsafe scenarios.

3.2 Simulation environment

A simulation environment in MATLAB and Simulink is set up in order to find when the safe and unsafe modes of the vehicle combination occurs. The environment makes use of the VTM library, containing the tractor semi-trailer combination, to simulate motion and dynamics between tractor, semi-trailer and road. The specific vehicle parameters used during simulations are presented in Appendix B.

3.2.1 Simulation scenario

A road profile is defined as the test track for the simulations. The track is initiated by a straight path of 20 m, followed by a 180 degree turn with radius R_r. The track ends with another straight of 20 m. Between the straights and the turn, transition parts of 15 m are added to avoid large instantaneous differences in road curvature which could generate large vehicle motion jerks. The path has no incline, decline or camber and consists of a single lane.

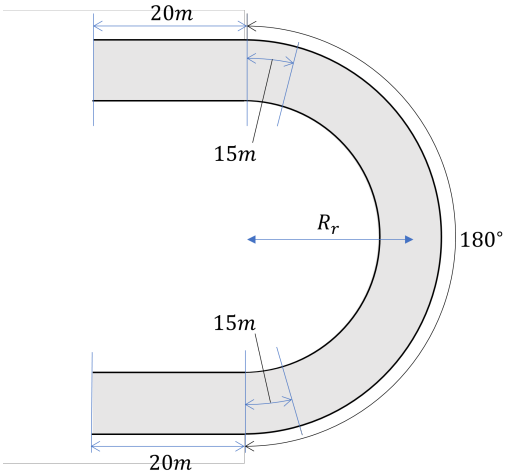

Figure 3.1: Road model used in simulations

The vehicle is initiated on the road at a set cruise speed which is controlled by the speed controller. The controller applies enough torque on the two rear axles of the tractor to keep the vehicle at the set speed.

Any occurrences of oscillations in the vehicle states, induced by the transition between the initial straight and the curve have to be canceled. Therefore the vehicle is run halfway through the track with the cruise controller acting on the first unit. Then, the speed controller is disconnected, letting the vehicle roll without any applied torque. Immediately after the disconnection, a fixed constant torque T is applied on each wheel on the two front axles of the trailer. Here, no traction control or slip control is used to limit the applied torque on the wheels.

3.2.2 Simulation parameters and data generation

In order for the SOE to manage all possible scenarios that the vehicle can be in, data from numerous different simulations are needed. There are many parameters that affect the vehicle's trajectory through a curve. For example the curve's radius, the velocity of the vehicle and the friction coefficient all play an important role when considering the motion of the vehicle and how it will be able to handle a curve. Thus, simulation data is needed for all possible combinations of such parameters in order to know how the vehicle will behave.

During simulations different combinations of longitudinal velocity v_x, friction coefficient between the tire and the road μ, curve radius R_r and applied trailer torque T are used. The friction coefficient is limited by its definition, which is the ratio between the frictional force resisting motion and the normal force between the surface and the object. The vehicle's velocity is upper limited by the standard speed limit on heavy goods vehicles without trailers (>3.5 metric tonnes) on motorways and expressways in Sweden at $25\frac{m}{s}$[19]. v_x is also limited by the maximum theoretical speed of the unit without slipping during a turn due to centripetal accelerations:

$$a_y = \frac{v_x^2}{R_r} = \mu g \implies v_{x,lim} = \sqrt{\mu g R_r} \tag{3.3}$$

The sum of applied wheel torque on the trailer, introduced in subsection 3.2.1, is bounded by the longitudinal slip limit between the four driven wheels of the trailer and the road

$$T_{x,2,tot} = (m_{2,1} + m_{2,2})g\mu r_2 \tag{3.4}$$

where $T_{x,2,tot}$ is the total applied torque on the driven wheels of the second unit in x-direction relative to its own coordinate frame and r_2 is the radius of the wheels on the second unit. Since only axles 2 and 3 are driven, the longitudinal slip limit is only considered for the axle loads for the driven axles.

By simulating different scenarios with different radii on the test track many different articulation angles are covered in the envelope. Simulations are performed using radii ranging from 10 m to 100 m.

To summarize, the limits of the parameters which make up the envelope are bounded as follows:

$$\begin{cases} \mu & \in [0,\ 1] \\ v_x & \in [0,\ \min(\sqrt{\mu g R_r},\ 25)] \\ T & \in [-\frac{1}{4}T_{x,2,tot},\ \frac{1}{4}T_{x,2,tot}] \\ R_r & \in [10,\ 100] \end{cases} \tag{3.5}$$

Each individual simulation run will generate one data point in the SOE, and depending on the outcome of the simulation it will be classified either as safe or unsafe. All generated data points contain relevant data from their corresponding simulation. This data is what the control system utilizes and is explained in detail in subsection 4.3.2 and subsection 4.3.4.

3.2.3 Estimations of vehicle states

When applying the torque on the trailer in the simulations, the current articulation angle θ and the coupling forces must be measured. These can be difficult to measure due to large jerks in the vehicle when applying the torque halfway through the track. Therefore, θ is approximated using the average of the last 30% of the measurements before the torque is applied. This will account for any fluctuations of θ close to when the torque is applied.

The coupling forces are affected by the applied torque on the trailer which in turn is delayed by the transfer function in Equation 2.1. The motors will exert the full torque requested within about 1 second. Similar as when approximating the articulation angle, another second of measurements are required to reach stable enough values of the coupling forces once the full torque of the trailer is applied to the vehicle. Therefore, the coupling forces are taken as the average values between 1 and 2 seconds after the torque is first applied to the trailer. If the vehicle does not manage to drive 2 seconds or more after the torque is applied, then the average is taken up until the end of the simulation. This will however increase the risk of uncertain and inaccurate estimations of the coupling forces.

3.3 Definition and setup of operating envelope

The idea of the safe operating envelope is to limit the driver's inputs to the vehicle to ensure safe driving. More specifically, by reading and analyzing the current states of the vehicle, the envelope can then be used as a reference to predict if the requests from the driver will result in safe vehicle motion. The objective is to create a point in the envelope with the current states of the vehicle, hereon denominated as "the state", and find a similar already existing point which is classified as safe. When such a point is found, the corresponding applied torque, T, associated with said point is set as the limit for the driver's inputs.

3.3.1 Envelope parameters and algorithm

There are several ways to define the data points and what they contain. One approach is to record the applied torque on each driven wheel of the trailer T as well as the friction coefficient between the tires and the road μ, the radius of the curve R_r and the longitudinal velocity of the tractor $v_{x,1}$. Since these are variables that may vary throughout the simulated curve they are recorded at the moment that the trailer torque is first applied. This results in a 4-dimensional envelope, that considers both vehicle states as well as environmental parameters. Each data point is classified with a flag depending on the outcome of the corresponding simulation.

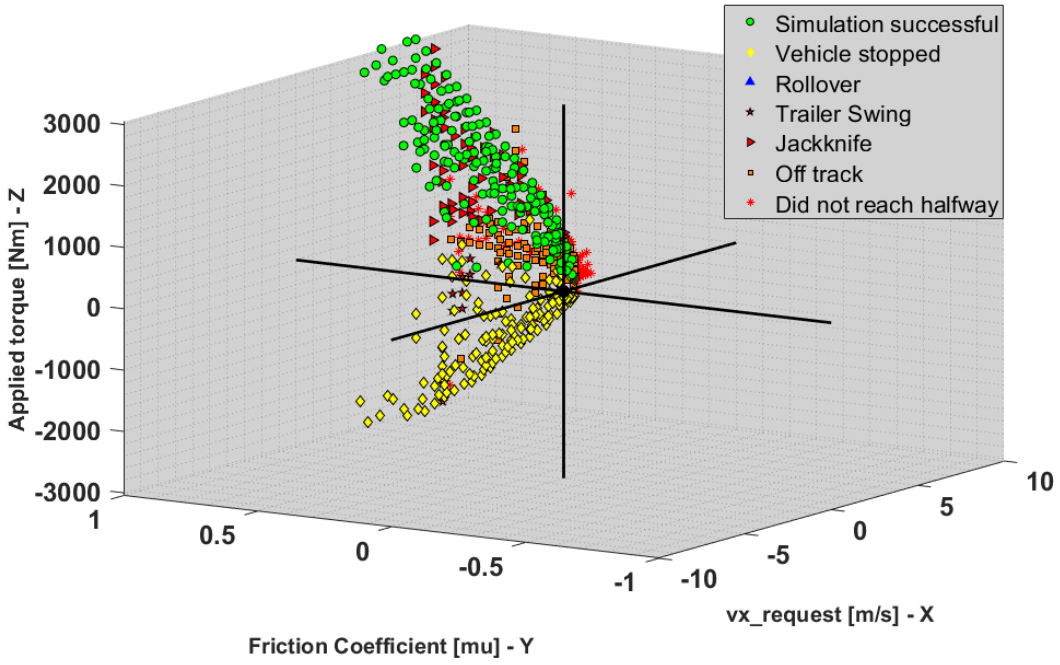

Figure 3.2: Visualization of 4-dimensional envelope consisting of T, $v_{x,1}$ and μ. Fixed radius of $R_r = 10$ m.

Figure 3.2 shows an example of data points gathered from a set of simulations, displayed in an isometric view. The simulations used a road profile with a radius of

$R_r = 10$ meters. In the figure each point is classified with a flag and a corresponding color.

This way of describing the envelope is useful when the parameters of the simulations are few and when the simulation environment on which the envelope is based is similar to the actual environment where the vehicle is to be used. Because of this, the 4-dimensional envelope will only be reliable when the trailer handles all propulsion and when radius of the road is known. However, since the dynamics of the vehicle will change depending on which units are used for propulsion, a more flexible definition of the envelope is needed in order to cover different propulsion distributions. Thus, the envelope must include additional parameters regarding to the state of the vehicle. By also including coupling forces $F_{cxr,1}$, $F_{cyr,1}$ in the envelope relations between the units can be made which allows for force limitations on either, or both of the two units. Furthermore, since the radius of the road is difficult to measure and not always a reliable metric of the pose of the vehicle, the road radius is replaced with the current articulation angle θ since it is easier to measure and makes for a better descriptor of the difference in yaw angle between tractor and trailer. Therefore, the parameters which define the envelope are instead chosen to be T, μ, $v_{x,1}$, $F_{cxr,1}$, $F_{cyr,1}$ and θ.

This way of representing the envelope will be more general since it is 6-dimensional and because the coupling forces allows for some degree of disturbance handling. For instance when the tractor is braking or when strong winds are pushing on the trailer the coupling forces will be affected, and thus such disturbances will also be considered by the control system.

The 6-dimensional envelope can be visualized by first considering it as a set of 3D spaces which are gathered in a 2D space. In the envelope, the parameters μ and $v_{x,1}$ are considered to vary the least out of the five parameters of the envelope which is why these are chosen to make up the 2D space. For each of the data points in the plane there exist a 3D space made up of the remaining parameters. This is depicted in Figure 3.3 where a point in the μ-v_x plane contains a set of points which are all classified according to the outcome of the simulation, as in the T-μ-$v_x - R_r$ envelope described earlier. Specifying all of the first five parameters then gives the specific data point's corresponding applied torque, which represents the last dimension. When implemented into a control system, the envelope works similar to a look-up table. The state of the vehicle is used as reference values for the first five parameters of the envelope: $\mu, v_{x,1}, \theta, F_{cx}$ and F_{cy}. These parameters then determine the corresponding torque limit.

To ensure that the envelope does not output a limit which could result in unsafe driving, i.e. a torque request which is too high or too low, some assumptions are made. It is assumed that a smaller μ, larger v_x, larger θ and larger absolute value of T individually and in combination with each other makes for a more difficult driving scenario and thus increases the likelihood for unsafe driving. Using the state of the vehicle as a reference the SOE algorithm will then find a similar data point of equal or higher difficulty level that has been classified as safe. The algorithm achieves this by methodically filtering out all points corresponding to easier driving scenarios. To

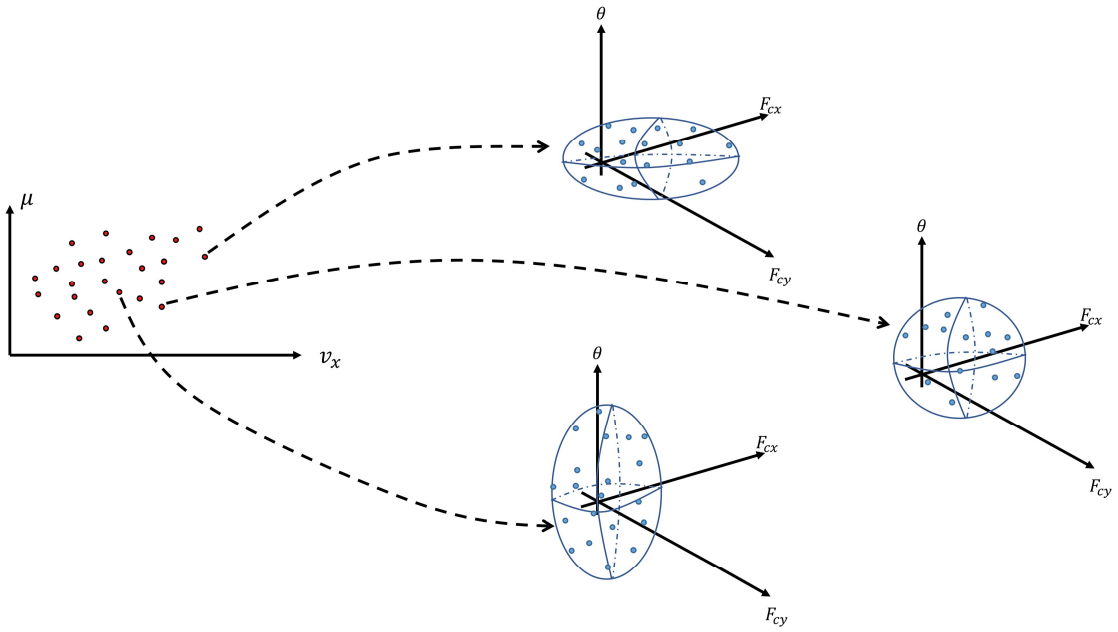

Figure 3.3: Visualization of the 6-dimensional SOE. A specific combination of μ, v_x, θ, F_{cx} and F_{cy} corresponds to an applied torque, T, representing the last dimension.

not limit the performance of the vehicle but at the same time include enough data points for the filtered subset, a small range of the chosen values of each parameter are used based on the assumptions made earlier

$$v_{x_{\text{current}}} \leq v_{x_{\text{chosen}}} \leq v_{x_{\text{current}}} + 1\frac{m}{s^2} \tag{3.6}$$

$$\mu_{\text{chosen}} = \max\{\mu_{\text{current}} \in \mu_e \mid \mu_{\text{chosen}} \leq \mu_{\text{current}}\} \tag{3.7}$$

$$\theta_{\text{current}} \leq \theta_{\text{chosen}} \leq \theta_{\text{current}} + 5°, \tag{3.8}$$

where μ_e is the set of friction coefficients used in the SOE. The algorithm of the SOE will find all safe data points corresponding to the current state of the vehicle, including the nearby points based on the assumptions in Equation 3.6-3.8. With only a subset of the entire envelope remaining, a nearest neighbor method using Euclidean distance is used to find the closest safe data point with regards to the current state. The torque corresponding to said data point is returned as a system limitation in terms of maximum positive and negative applicable torque of the trailer, $\overline{T}$ and $\underline{T}$. Since the envelope is highly non-linear, no interpolation between existing points are made since this could result in a wrong assumption about whether the state is safe or not. Since only the safe points in the envelope are interesting when limiting the trailer, the unsafe points are removed from the envelope to decrease the number of points to process which decreases the computational time of the envelope.

With only the safe points remaining in the envelope, Figures 3.4-3.6 are used to show the effect of changing friction coefficient μ in the F_{cx}-F_{cy}-θ-space. The data points displayed include all values of $v_{x,1}$ and T included in the envelope for the chosen μ. As expected and as assumed earlier, larger values of μ allows for larger longitudinal and lateral coupling forces.

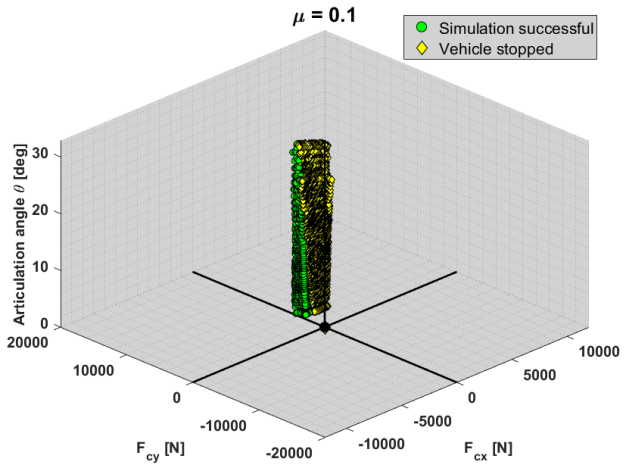

Figure 3.4: Safe points in SOE with $\mu = 0.1$, $\forall v_x$. 15223 data points

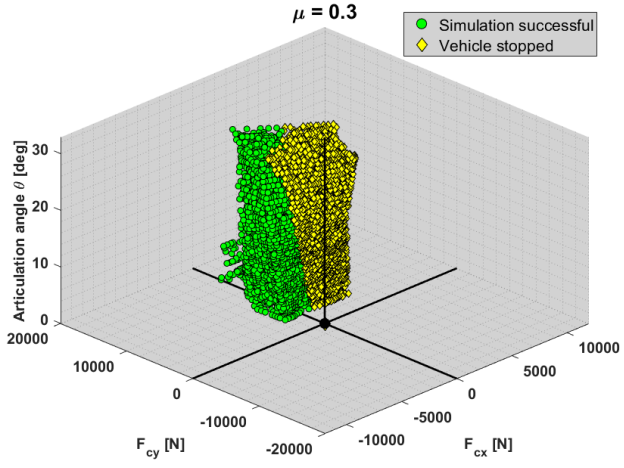

Figure 3.5: Safe points in SOE with $\mu = 0.3$, $\forall v_x$. 8853 data points

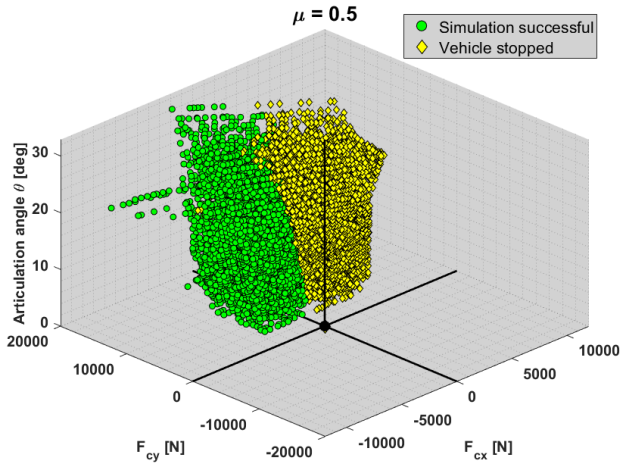

Figure 3.6: Safe points in SOE with $\mu = 0.5$, $\forall v_x$. 9028 data points

Algorithm 1 shows the concept of how the SOE can limit the inputted torque, expressed as pseudo-code. Variables from the current state of the vehicle has their last index as "s" and the variables belonging to the envelope has their last index as "e".

Algorithm 1 Limiting T using a safe operating envelope

Input: v_{x_s},μ_s,F_{cx_s},F_{cy_s},$|\theta_s|$,T_s,E ▷ Input variable E contains envelope
Output: $\overline{T}, \underline{T}$

```
μ ← max(μ_s < μ_e)
E ← Remaining points in E with μ_e = μ
E ← Remaining points in E with v_xs ≤ v_xe ≤ v_xs + 1
E ← Remaining points in E with θ_s ≤ θ_e ≤ θ_s + 5
dists ← ‖E − [F_cxs, F_cys]‖                    ▷ Euclidean distance
neighbors ← Index after sort of dists in ascending order
n ← 1                                           ▷ Neighbor index
while n ≤ N_neighbors do
    if T_s ≥ 0 and E(neighbor_n)_T ≥ 0 then
        F_cx_safe ← neighbor_{n,Fcx}
        F_cy_safe ← neighbor_{n,Fcy}
    else if T_s < 0 and E(neighbor_n)_T < 0 then
        F_cx_safe ← neighbor_{n,Fcx}
        F_cy_safe ← neighbor_{n,Fcy}
    else
        n ← n + 1
    end if
end while
T_safe ← E(neighbor_n)_T
if T_safe ≥ 0 then
    T̄ ← T_safe
    T̲ ← −Inf
else
    T̲ ← T_safe
    T̄ ← Inf
end if
```

3.3.2 Creation of envelope and optimizing of simulations

The resolution of the envelope increases by the number of simulations and resulting data points. A very high resolution of the envelope is desirable as it allows for identifying unsafe scenarios more accurately and will find more suitable suggestions of torque limits as to maximize performance. On the contrary, using a large envelope will require more computing resources in order to find the closest safe data point. In order to obtain a SOE which covers all relevant states of the vehicle the aforementioned parameter limits in Equation 3.5 are used. The envelope created for the sake of this thesis includes 393600 data points. These data points corresponds to simulations including 48 different road profiles, each simulated using 10 different friction coefficients, 20 different velocities and 41 different applied torques.

Since each simulation runs for an average of approximately 120 seconds, obtaining a high fidelity envelope on a medium range consumer grade computer would require several months to complete the simulations. Because of this, the simulations are optimized for parallel computing using the Parallel Computing toolbox for MATLAB and executed on the computer cluster Vera, located at Chalmers University of Technology. By using the toolbox together with the computer cluster, several parallel simulations can be run simultaneously and the total simulation time can be greatly reduced.

4

Control system

This chapter addresses the control system used to translate the drivers input to actuator signals. Vehicle combinations contain several individually controllable units and each unit contains several individually controllable actuators. Thus, sophisticated control strategies are required in order to distribute the control signals in an efficient manner.

4.1 Control allocation theory

Using a trailing unit, such as a semi-trailer for propulsion may contribute negatively to the stability of the vehicle combination, particularly the yaw stability. There is an increased risk of unwanted and dangerous vehicle behaviors such as jackknifing and trailer swing. The stability of the vehicle may be improved by using the actuator limiting SOE in conjunction with control allocation algorithms. Control allocation with a weighted least squares (WLS) solver can be used to solve the optimization issue of distributing actuator signals on a heavy multi-unit vehicle which is a popular and well studied method [20]–[24].

4.1.1 Background

In control system applications the goal is to translate some set of input signals into a desired behavior of the system which should be controlled. This is often achieved by deriving a mathematical model of the system in the form of a state space representation:

$$\dot{\boldsymbol{x}} = f(\boldsymbol{x}, \boldsymbol{u}) \tag{4.1}$$

The states of the system is represented by $\boldsymbol{x} \in \mathbb{R}^n$ and their corresponding time derivatives is $\dot{\boldsymbol{x}}$. Input signals to the system are represented by $\boldsymbol{u} \in \mathbb{R}^m$ and the rate of change in system states is described by the, possibly nonlinear, function $f(\cdot)$. The state space representation can however often be replaced by a less complex approximation:

$$\dot{\boldsymbol{x}} = g(\boldsymbol{x}) + h(\boldsymbol{x})\boldsymbol{u} \tag{4.2}$$

Control allocation is a control strategy that uses state space representations in order to control over-actuated systems. In such systems the number of control inputs, m, exceed the number of controlled system states, n [25]. In this case there exists more than one combination of input signals, $\boldsymbol{u}$, that can realize the desired behavior of the

system. Such systems can be dealt with by implementing a virtual control signal, $\boldsymbol{v} \in \mathbb{R}^n$, which gives the state space representation:

$$\dot{\boldsymbol{x}} = g(\boldsymbol{x}) + \boldsymbol{v} \tag{4.3}$$

Since $dim(\boldsymbol{v}) = dim(\boldsymbol{x})$, the virtual control signal that can realize a specific desired behavior will be unique. The virtual control signal will be related to the actuator signals according to

$$\boldsymbol{v} = B\boldsymbol{u} \tag{4.4}$$

where $B \in \mathbb{R}^{n \times m}$ is the control efficiency matrix which, in order to be able to solve for $\boldsymbol{u}$, is a linear approximation of $h(\boldsymbol{x})$. Given a B-matrix that maps the actuator control signals into virtual control signals, the control allocation problem is reduced to finding the optimal set of actuator signals that yields the desired virtual signals.

4.1.2 Optimization

Despite the uniqueness of the virtual control signal, $\boldsymbol{v}$, there may still exist several sets of actuator signals that fulfills Equation 4.4. There are different ways of solving this optimization problem [26] but a common way to find the most optimal $\boldsymbol{u}$ is to use the constrained sequential least squares (SLS) formulation [25], [27], [28]

$$\begin{aligned} \boldsymbol{u} &= \arg\min_{\boldsymbol{u} \in \Omega} ||W_u(\boldsymbol{u}_{des} - \boldsymbol{u})||_2^2 \\ \Omega &= \arg\min_{\underline{\boldsymbol{u}} \leq \boldsymbol{u} \leq \overline{\boldsymbol{u}}} ||W_v(B\boldsymbol{u} - \boldsymbol{v})||_2^2 \end{aligned} \tag{4.5}$$

which can be simplified to the weighted least squares (WLS) problem:

$$\boldsymbol{u} = \arg\min_{\underline{\boldsymbol{u}} \leq \boldsymbol{u} \leq \overline{\boldsymbol{u}}} (||W_u(\boldsymbol{u}_{des} - \boldsymbol{u})||_2^2 + \gamma ||W_v(B\boldsymbol{u} - \boldsymbol{v})||_2^2) \tag{4.6}$$

Here, the actuator signals are constrained by their upper and lower limitations, $\overline{\boldsymbol{u}}$ and $\underline{\boldsymbol{u}}$. W_u and W_v are weighting matrices used to prioritize minimization of certain actuator signals and virtual control signals. $\boldsymbol{u}_{des}$ are the desired input signals and γ is a scaling parameter for changing priority between actuator signals and virtual control signals during the optimization.

There are different aspects to consider when choosing the tuning parameters in Equation 4.6. Prioritizing $\boldsymbol{v} = B\boldsymbol{u}$ more than the input signal error allows for larger deviations in $\boldsymbol{u}_{des} - \boldsymbol{u}$ which could be less energy-efficient. On the contrary, if the input signal error is prioritized more, minimizing the actuator usage is prioritized. This may be a more energy efficient solution that also may result in undesired vehicle motion since $B\boldsymbol{u}$ may deviate from $\boldsymbol{v}$.

4.2 Combination level control allocation

In order to coordinate and control the movement of the whole vehicle combination a control allocator system is introduced. The combination level control allocator receives inputs in the form of requested global forces on the vehicle $\boldsymbol{v}_c$ from a driver

model. It then outputs the distribution of forces on each of the two units in $\boldsymbol{u}_c$ to achieve the requested global forces. These are, for a tractor semi-trailer vehicle combination, suitably chosen as

$$\boldsymbol{v}_c = \begin{bmatrix} F_{x,req} & F_{y,req} & M_{z,1,req} & M_{z,2,req} \end{bmatrix} \tag{4.7}$$

$$\boldsymbol{u}_c = \begin{bmatrix} F_{x_{V,1,em}} & F_{x_{V,1,sb}} & F_{y_{V,1}} & M_{z_{V,1}} & F_{x_{V,2,em}} & F_{x_{V,2,sb}} & F_{y_{V,2}} & M_{z_{V,2}} \end{bmatrix} \tag{4.8}$$

where subscript "1" refers to the first unit and "2" refers to the second unit. The chosen virtual signals and input signals allows for control of the total requested longitudinal and lateral forces, $F_{x,req}$ and $F_{y,req}$, applied on the vehicle as well as control of each unit's moment around their COGs which is desirable when for instance the vehicle is turning and each unit must rotate enough to not cut corners and end up in the opposite road lane.

Note that the longitudinal force is also split into two forces, one produced by the electrical motors (which can be either propelling or braking) and one pure braking force produced by the service brakes.

4.2.1 Translation of driver inputs to allocator

The inputs from the driver $a_{x,req}$ and $\delta_{11,req}$ as explained in chapter 2 must be converted into the chosen virtual control signals $\boldsymbol{v}_c$ before the combination level control allocator can use them. The strategy used when determining what translation needs to be done to the driver inputs is that the equations that make up $\boldsymbol{v}_c$ must be equivalent to the corresponding equations in the control allocators of the systems. This will allow for the WLS solver to accurately find the optimal solution with the given inputs and minimizing the errors between the optimal input signals multiplied with the control efficiency matrices and the virtual control signals as $B\boldsymbol{u} - \boldsymbol{v}$.

The requested longitudinal acceleration is readily translated to a requested longitudinal force by multiplying itself with the total mass of the vehicle according to Newton's second law of motion:

$$F_{x,req} = a_{x,req} m_{tot} \tag{4.9}$$

However, this requested force will not be sufficient to accelerate the vehicle to the desired $a_{x,req}$ since motion resistance forces as air resistance and rolling resistance will decelerate the vehicle. These forces must therefore be compensated by estimating and adding them to the total requested longitudinal force on the vehicle. Using Equation 2.7 and 2.10, Equation 4.9 can be rewritten to compensate for resistive forces:

$$F_{x,req} = a_{x,req} m_{tot} + F_d + F_{roll,tot} \tag{4.10}$$

Now the requested lateral force on the vehicle must be translated from $\delta_{11,req}$. As the tire model used in the simulation environment is complex and highly nonlinear a simpler tire model estimation must be done in order to relate the steering angle of the wheels on the front axle to the lateral forces exerted on them. By using a simplified tire force model the equations can also be used in the truck unit control allocator in order to properly match the equations as explained in the beginning of this section.

A linear tire force model is chosen where the steering angle is proportional to the lateral forces, together with a tire cornering stiffness factor C_{11}:

$$F_{y,req} = C_{11}\delta_{11} \tag{4.11}$$

Again, only one steering angle is used to describe both wheels since they are assumed to be mechanically linked together.

Using $F_{y,req}$, the requested moment about the first unit is readily calculated as:

$$M_{z,1,req} = F_{y,req}\, l_{a,11} \tag{4.12}$$

To allow for the trailing unit to follow a similar trajectory as the leading unit and regarding rotation about the z-axis, the requested moment about the second unit is the same as for the first unit but delayed. The delay is time varying and is dependent on the speed of rear axle of the first unit and the length of the second unit. This can be described by considering the requested moments as functions dependent on time

$$M_{z,2,req}(t) = M_{z,1,req}(t - \tau(t)) \tag{4.13}$$

where the time delay function is described as:

$$\tau(t) = \frac{d_{r1} + d_{f2}}{\sqrt{v_{x,13}^2 + v_{y,13}^2}} \tag{4.14}$$

4.2.2 Control efficiency matrix B_c

The control efficiency matrices are responsible for the translation of the driver inputs to the vehicle to the actuator usage through $B\boldsymbol{u} = \boldsymbol{v}$. To construct the B-matrices the dynamics of the vehicle must be known and described as a function with respect to the actuator usage. Using Newtonian mechanics, equations of motion of the entire vehicle can be set up as:

$$\begin{cases} F_{x,1} = m_1 a_{x_1} & = F_{x_{V,1,em}} + F_{x_{V,1,sb}} - F_{xcr_1} - F_{res,1} \\ F_{y,1} = m_1 a_{y_1} & = F_{y_{V,1}} - F_{ycr_1} \\ M_{z,1} = J_1 \dot{\omega}_{z_1} & = M_{z_{V,1}} + F_{ycr_1} d_{r_1} \\ \\ F_{x,2} = m_2 a_{x_2} & = F_{x_{V,2,em}} + F_{x_{V,2,sb}} - F_{xcr_1}\cos\theta_1 \\ & \quad + F_{ycr_1}\sin\theta_1 - F_{res,2} \\ F_{y,2} = m_2 a_{y_2} & = F_{y_{V,2}} - F_{xcr_1}\sin\theta_1 - F_{ycr_1}\cos\theta_1 \\ M_{z,2} = J_2 \dot{\omega}_{z_2} & = M_{z_{V,2}} - F_{xcr_1}\sin\theta_1 d_{f_2} \\ & \quad - F_{ycr_1}\cos\theta_1 d_{f_2} \end{cases} \tag{4.15}$$

Complete derivations and equations are found in Appendix A.1 and the complete matrix for the allocator is:

$$B_c = \begin{bmatrix} 1 & 1 & 0 & 0 & \cos\theta_1 & \cos\theta_1 & \sin\theta_1 & 0 \\ 0 & 0 & 1 & 0 & -\sin\theta_1 & -\sin\theta_1 & \cos\theta_1 & 0 \\ 0 & 0 & 0 & 1 & d_{r_1}\sin\theta_1 & d_{r_1}\sin\theta_1 & -d_{r_1}\cos\theta_1 & 0 \\ 0 & 0 & 0 & 0 & 0 & 0 & d_{f_2} & 1 \end{bmatrix} \tag{4.16}$$

4.2.3 Capabilities of global forces

The global forces $\boldsymbol{v}_c$ are divided among the two units through control allocation where $\boldsymbol{u}_c$ contains the requested forces on each unit $\boldsymbol{v}_1$ and $\boldsymbol{v}_2$[1]. However because of limitations regarding slip conditions, power and torque limitations on motors and other supporting algorithms[2], each unit can not always deliver what is requested from the combination control allocator. To account for this, each unit provides capabilities to the combination control allocator of what upper and lower bounds of $\boldsymbol{v}_1$ and $\boldsymbol{v}_2$ they are capable of delivering. The controller then reallocates the global forces using the capabilities from each unit as per the WLS problem in Equation 4.6.

The capabilities $\overline{\boldsymbol{v}}$ and $\underline{\boldsymbol{v}}$ from each unit are calculated using their respective control efficiency matrices and their limits $\underline{\boldsymbol{u}}_1$, $\overline{\boldsymbol{u}}_1$, $\underline{\boldsymbol{u}}_2$ and $\overline{\boldsymbol{u}}_2$ as:

$$\overline{\boldsymbol{v}}_1 = B_1 \overline{\boldsymbol{u}}_1 \tag{4.17}$$
$$\underline{\boldsymbol{v}}_1 = B_1 \underline{\boldsymbol{u}}_1 \tag{4.18}$$
$$\overline{\boldsymbol{v}}_2 = B_2 \overline{\boldsymbol{u}}_2 \tag{4.19}$$
$$\underline{\boldsymbol{v}}_2 = B_2 \underline{\boldsymbol{u}}_2 \tag{4.20}$$

4.3 Unit level control allocation

For a long vehicle combination with more than one unit there are usually actuators on each unit. Modern commercial vehicle combinations generally use the actuators of the first unit for propulsion and braking, while the actuators on the upcoming units are only used for braking. This makes for a simple control strategy since each unit is only responsible for braking its own weight during deceleration and all but the first unit is passive while accelerating. However, when e-trailers becomes a reality in the future, all units may be used for both propulsion and braking. This requires each unit to be able to control its own motion in order to fulfill the driver's desires regarding vehicle heading and velocity. This can be done by implementing unit specific control allocators, that can realize a requested virtual signal by using a unit specific control efficiency matrix, B_i.

4.3.1 Control efficiency matrices B_1 and B_2

With the allocated forces from the combination level control allocator in $\boldsymbol{u}_c$, each unit must allocate actuator usage in order to achieve the desired motion. The virtual control signals are naturally set as $\boldsymbol{v}_1$ and $\boldsymbol{v}_2$ since $\boldsymbol{u}_c \subseteq [\boldsymbol{v}_1, \boldsymbol{v}_2]$ and the input signals

[1] Choice of virtual control signal for each unit are provided in section 4.3
[2] These limitations are further explained in subsection 4.3.2

includes all of the available actuators on the tractor and trailer respectively:

$$\boldsymbol{v}_1 = \begin{bmatrix} F_{x_{V,1,em}} & F_{x_{V,1,sb}} & F_{y_{V,1}} & M_{z_{V,1}} \end{bmatrix} \tag{4.21}$$

$$\begin{aligned} \boldsymbol{u}_1 = \Big[& T_{11L,em} \quad T_{11R,em} \quad T_{12L,em} \quad T_{12R,em} \quad T_{13L,em} \quad T_{13R,em} \quad \dots \\ & T_{11L,sb} \quad T_{11R,sb} \quad T_{12L,sb} \quad T_{12R,sb} \quad T_{13L,sb} \quad T_{13R,sb} \quad \delta_{11} \Big] \end{aligned} \tag{4.22}$$

$$\boldsymbol{v}_2 = \begin{bmatrix} F_{x_{V,2,em}} & F_{x_{V,2,sb}} & F_{y_{V,2}} & M_{z_{V,2}} \end{bmatrix} \tag{4.23}$$

$$\begin{aligned} \boldsymbol{u}_2 = \Big[& T_{21L,em} \quad T_{21R,em} \quad T_{22L,em} \quad T_{22R,em} \quad T_{23L,em} \quad T_{23R,em} \quad \dots \\ & T_{21L,sb} \quad T_{21R,sb} \quad T_{22L,sb} \quad T_{22R,sb} \quad T_{23L,sb} \quad T_{23R,sb} \Big] \end{aligned} \tag{4.24}$$

The control efficiency matrices and their complete derivations are shown in Appendix A.2-A.3.

4.3.2 Actuator limits

The installed actuators on the vehicle units include electric motors, mechanical service brakes and steered wheel axles. The purpose of finding the actuator limitations of the vehicle units is to be able to calculate the capabilities of each unit in order to control the plant model properly. Limits on the installed actuators depend on physical limits, the SOE of the trailer and supporting algorithms such as brake blending[3].

All installed actuators of the same type on the vehicle have the same properties. The limits of the electrical motors are limited by their torque and power ratings and are set as:

$$\overline{T}_{em} = \quad 6500 \quad [\text{Nm}] \tag{4.25}$$

$$\underline{T}_{em} = -6500 \quad [\text{Nm}] \tag{4.26}$$

$$\overline{P}_{em} = 125000 \quad [\text{W}] \tag{4.27}$$

$$\underline{P}_{em} = -125000 \quad [\text{W}] \tag{4.28}$$

It is assumed that the torque output from the electric motors is proportional to the power usage of each motor. It is also assumed that the motors and the corresponding wheels are directly connected without any gearing. Therefore, the torque on each motor limited by its power rating is

$$\overline{T}_{P,ijs} = \frac{\overline{P}_{em}}{|\omega_{w,ijs}|} \tag{4.29}$$

$$\underline{T}_{P,ijs} = \frac{\underline{P}_{em}}{|\omega_{w,ijs}|} \tag{4.30}$$

where $\omega_w = \omega_m$ is the rotational speed of the wheel and the rotational speed of the motor respectively. The electrical motors are also limited by the frictional limit

[3]Introduced in subsection 4.3.3

between tire and road as to not apply a torque which would make the wheels slip. This limit is defined as

$$\overline{T}_{\mu,ijs} = \frac{1}{2} m_{ij} g \mu r_i \tag{4.31}$$

$$\underline{T}_{\mu,ijs} = -\frac{1}{2} m_{ij} g \mu r_i \tag{4.32}$$

It is assumed that the normal load on each axle is evenly distributed between the left and right wheel. The final actuator limits on the electric motors are the combinations of each of the three limits in Equations 4.25-4.32 as:

$$\overline{\boldsymbol{u}}_{em,ijs} = \min(\overline{T}_{em}, \overline{T}_{P,ijs}, \overline{T}_{\mu,ijs}) \tag{4.33}$$

$$\underline{\boldsymbol{u}}_{em,ijs} = \max(\underline{T}_{em}, \underline{T}_{P,ijs}, \underline{T}_{\mu,ijs}) \tag{4.34}$$

The service brakes are assumed to only be limited by the lower frictional torque limit between tire and road as to avoid locking the tires when braking. The service brakes can not apply a positive torque on the wheels, thus the limits of the service brakes are:

$$\overline{T}_{sb,ijs} = \overline{\boldsymbol{u}}_{sb,ijs} = 0 \tag{4.35}$$

$$\underline{T}_{sb,ijs} = \underline{\boldsymbol{u}}_{sb,ijs} = \underline{T}_{\mu,ijs} \tag{4.36}$$

The steering angle δ_{11} is considered as one actuator. Since it is only supposed to support the driver by making minor adjustments to the driver's desired steering angle, it is limited as

$$\overline{\boldsymbol{u}}_{\delta_{11}} = \delta_{11} + \delta_u \tag{4.37}$$

$$\underline{\boldsymbol{u}}_{\delta_{11}} = \delta_{11} - \delta_u \tag{4.38}$$

where $\delta_u = 1°$.

Now the control system consist of control allocators on combination and unit levels together with actuator limitations which takes driver requests as inputs and outputs actuator signals to a plant model. Figure 4.1 shows a conceptual block diagram of the control system architecture.

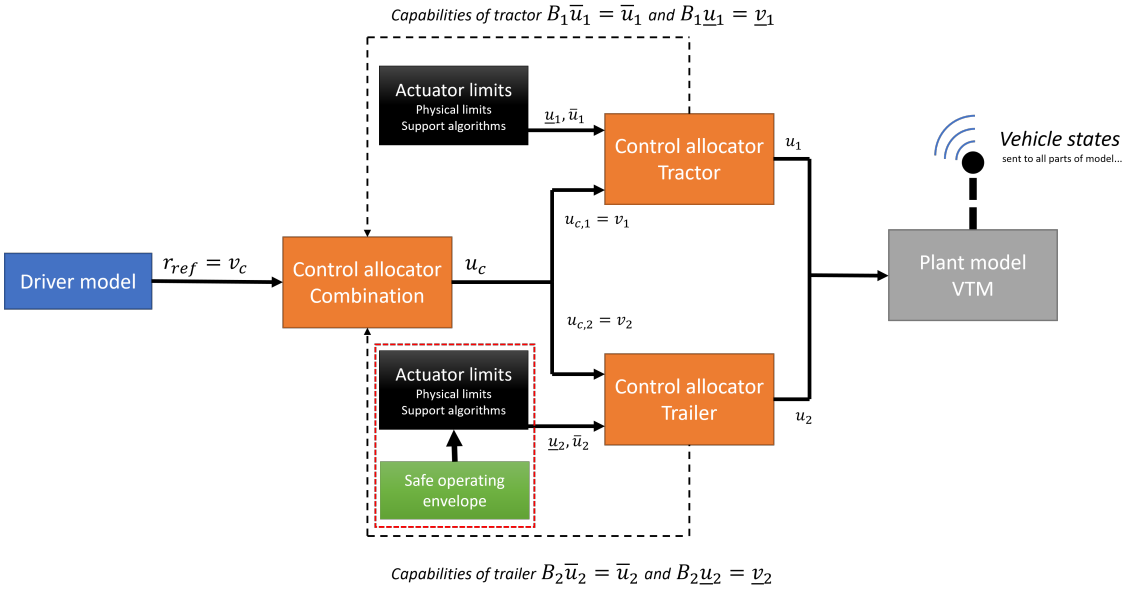

Figure 4.1: Conceptual architecture of implemented control system

4.3.3 Brake blending algorithm

Since electric trucks have two brake systems, e-motor braking and mechanical service brakes, different braking strategies can be implemented in order to prioritize either one of them. One strategy is to implement a ratio that for example applies 60% of the requested brake torque to the e-motors and 40% to the service brakes. However, the total braking torque of the two brake systems must still not surpass $\underline{T}_{\mu,ijs}$ from Equation 4.32, even though the actuators limits allow for higher applied torque. Another thing to consider is when the e-motors can be used for braking. When using the e-motors for braking they are recuperating energy to the batteries and if the batteries' state of charge (SoC) is too high the e-motors cannot be used. Using the e-motors for braking in this case might result in damaged batteries. In order to solve the issues with having two individual brake systems with different properties, a brake blending algorithm is developed. The algorithm uses the actuator limits from subsection 4.3.2 together with the current SoC of the batteries.

The brake blending algorithm can be seen in Algorithm 2. Inputs to the algorithm are the vector of actuator limits, $\underline{\boldsymbol{u}}$, and the vector of applicable brake torque limits for each wheel before losing traction, $\underline{\boldsymbol{T}}_{\mu}$. Other inputs are the current SoC of the battery together with its maximum value as well as the requested ratio of e-motor braking relative to service brakes, η. A ratio of 1 means that all brake torque should come from the e-motors.

For the tractor unit the actuator limits used in the control allocator will be the output of the brake blending algorithm. These will be used during the WLS optimization step in the control allocator. However, the actuator limits of the trailer will be constrained further by using the SOE from chapter 3, detailed in subsection 4.3.4.

Algorithm 2 Brake blending

Input: η, $\underline{\boldsymbol{u}}$, $\underline{\boldsymbol{T}}_{\mu,k}$, SoC, $\overline{SoC}$
Output: $\underline{\boldsymbol{u}}$
$\underline{\boldsymbol{u}} \subseteq \begin{bmatrix} \underline{\boldsymbol{u}}_{em} & \underline{\boldsymbol{u}}_{sb} \end{bmatrix}$
for $k \leftarrow$ each wheel of unit **do**
  if $(\underline{u}_{em,k} + \underline{u}_{sb,k}) \leq \underline{\boldsymbol{T}}_{\mu,k}$ and $SoC < \overline{SoC}$ **then**
    Brake capability is higher than friction limit
    $\overline{\eta}_{sb} \leftarrow \frac{\underline{u}_{sb,k}}{\underline{\boldsymbol{T}}_{\mu,k}}$
    $\overline{\eta}_{em} \leftarrow \frac{\underline{u}_{em,k}}{\underline{\boldsymbol{T}}_{\mu,k}}$
    if $\overline{\eta}_{em} < \overline{\eta}_{sb}$ **then**
      Electric motor brake is limiting
      if $\overline{\eta}_{em} \geq \eta$ **then**
        $\underline{u}_{em,k} \leftarrow \eta \underline{\boldsymbol{T}}_{\mu,k}$
        $\underline{u}_{sb,k} \leftarrow (1-\eta)\underline{\boldsymbol{T}}_{\mu,k}$
      else
        $\underline{u}_{em,k} \leftarrow \overline{\eta}_{em} \underline{\boldsymbol{T}}_{\mu,k}$
        $\underline{u}_{sb,k} \leftarrow (1-\overline{\eta}_{em})\underline{\boldsymbol{T}}_{\mu,k}$
      end if
    else
      Service brake is limiting
      if $\overline{\eta}_{sb} \geq (1-\eta)$ **then**
        $\underline{u}_{em,k} \leftarrow \eta \underline{\boldsymbol{T}}_{\mu,k}$
        $\underline{u}_{sb,k} \leftarrow (1-\eta)\underline{\boldsymbol{T}}_{\mu,k}$
      else
        $\underline{u}_{em,k} \leftarrow (1-\overline{\eta}_{sb})\underline{\boldsymbol{T}}_{\mu,k}$
        $\underline{u}_{sb,k} \leftarrow \overline{\eta}_{sb} \underline{\boldsymbol{T}}_{\mu,k}$
      end if
    end if
  else if $(\underline{u}_{em,k} + \underline{u}_{sb,k}) > \underline{\boldsymbol{T}}_{\mu,k}$ and $SoC < \overline{SoC}$ **then**
    Brake capability is lower than friction limit
    $\underline{u}_{em,k} \leftarrow \underline{u}_{em,k}$
    $\underline{u}_{sb,k} \leftarrow \underline{u}_{sb,k}$
  else
    Brake capability is lower than friction limit, $\overline{SoC}$ *reached*
    $\underline{u}_{em,k} \leftarrow 0$
    $\underline{u}_{sb,k} \leftarrow \underline{u}_{sb,k}$
  end if
end for

4.3.4 Contribution from SOE to actuator limits

The SOE, defined and explained in chapter 3, provides upper and lower limits of the total applied torques on the wheels of the trailer which still ensures safe driving. The defined actuator limits $\overline{\boldsymbol{u}}_2$ and $\underline{\boldsymbol{u}}_2$ derived from earlier sections must be further limited as to include the limits from the SOE. Since the SOE does not limit each

wheel of the trailer individually, a method of reducing the total applied torque must be established. The idea is to compare the total applied torque on the trailer with the limits from the SOE, $\overline{T}$ and $\underline{T}$, and changing the applied torque on each wheel with a common factor which adjusts the total actuator usage as to comply with the more strict limits of the envelope.

$$\overline{\boldsymbol{u}}_2 = \begin{cases} \frac{\overline{\boldsymbol{u}}_2 \overline{T}_{SOE}}{\Sigma \overline{\boldsymbol{u}}_2} & \text{if } \sum \overline{\boldsymbol{u}}_2 > \overline{T}_{SOE} \\ \overline{\boldsymbol{u}}_2 & \text{otherwise} \end{cases} \tag{4.39}$$

$$\underline{\boldsymbol{u}}_2 = \begin{cases} \frac{\underline{\boldsymbol{u}}_2 \underline{T}_{SOE}}{\Sigma \underline{\boldsymbol{u}}_2} & \text{if } \sum \underline{\boldsymbol{u}}_2 < \underline{T}_{SOE} \\ \underline{\boldsymbol{u}}_2 & \text{otherwise} \end{cases} \tag{4.40}$$

This will adjust all the applied torque on the actuators (if the first conditions in Equation 4.39 and 4.40 are fulfilled) such that $\sum \overline{\boldsymbol{u}}_2 = \overline{T}$ and $\sum \underline{\boldsymbol{u}}_2 = \underline{T}$.

4.4 Energy utilization optimization

One of the main issues and motivations of the thesis is to optimize the energy usage on the vehicle in order to maximize the total range traveled. Some energy optimization can be done by choosing appropriate weight matrices in the control allocators as described in the WLS formulation in Equation 4.6, choosing suitable scaling parameters γ and by adjusting the desired input control signals $\boldsymbol{u}_{des}$ to favor low energy usage on the vehicle.

When choosing appropriate weight matrices, the general strategy presented in this section is to realize that all kinetic energy is lost through heat dissipation when using the service brakes and that the electric motors can regenerate 90% of the kinetic energy of the truck [29] in ideal conditions. The input control signal weight matrices in the unit level control allocators $W_{u,1}$ and $W_{u,2}$ are therefore chosen as

$$W_{u,1} = \text{diag}\begin{bmatrix} 0.1 & 0.1 & 0.1 & 0.1 & 0.1 & 0.1 & 1 & 1 & 1 & 1 & 1 & 1 & 1 \end{bmatrix} \tag{4.41}$$

$$W_{u,2} = \text{diag}\begin{bmatrix} 0.1 & 0.1 & 0.1 & 0.1 & 0.1 & 0.1 & 1 & 1 & 1 & 1 & 1 & 1 \end{bmatrix} \tag{4.42}$$

where the use of the electric motors are rewarded by a factor of 10 compared to the service brakes. Also, the steering angle δ_{11} is also given the same weight in $W_{u,1}$ as the service brake actuators.

The control allocators may find solutions to the WLS problem which achieves the desired motions of the vehicle but in an energy-inefficient way. This can be achieved for instance by allowing some actuators on a unit to apply negative longitudinal forces and some to apply counteracting positive longitudinal forces. To avoid this the novel solution of choosing $\boldsymbol{u}_{des,1} = \boldsymbol{0}$ and $\boldsymbol{u}_{des,2} = \boldsymbol{0}$ the solver will reward minimal actuator usage and therefore avoiding any actuator counteracting each other within each unit.

In the combination level control allocator, it is desired to not have the global forces on each on the two vehicle units counteracting each other. Here the novel solution

of letting $\boldsymbol{u}_{des,c} = \mathbf{0}$ is not a sufficient condition for the desired input control signal as the force distribution between the units is dependent of the desired motion of the vehicle. Therefore an algorithm is implemented where $\boldsymbol{u}_{des,c}$ is chosen depending on the desired forces from the driver together with the capabilities of the units. The purpose of the algorithm is to distribute longitudinal forces in $\boldsymbol{u}_{des,c}$ according to the unit distribution vector $\boldsymbol{\lambda} = [\lambda_1, \lambda_2]$ and the brake force distribution vector $\boldsymbol{\kappa} = [\kappa_{em}, \kappa_{sb}]$. Here, $\boldsymbol{\lambda}$ determines how the longitudinal force requested is to be split up between the tractor and semi-trailer such that $0 \leq \lambda_i \leq 1$ and $\lambda_1 + \lambda_2 = 1$. Similarly, $\boldsymbol{\kappa}$ determines the desired split of the brake force between the electric motors and the service brakes such that $0 \leq \kappa_i \leq 1$ and $\kappa_{em} + \kappa_{sb} = 1$.

First it is determined if the requested longitudinal force on the vehicle is positive. In that case, the force desired on the electric motors on the units are allotted a split of $F_{x,req}$ unless the capabilities of the electric propelling force on the units are lower than the respective splits of $F_{x,req}$ in which case the capabilities determine the desired forces on the electric propulsion forces.

If the requested longitudinal force on the vehicle is negative however, the total brake force is first split on the two units and then the brake forces from the electric motors and service brakes are split on each unit. The way of splitting the forces on each unit and then on each longitudinal force within each unit is done in the same manner as for when determining the split of propelling forces on the vehicle as described earlier. Algorithm 3 describes the dynamic selection of the desired force distribution in a combination level control allocator as implemented in the system depicted in Figure 4.2.

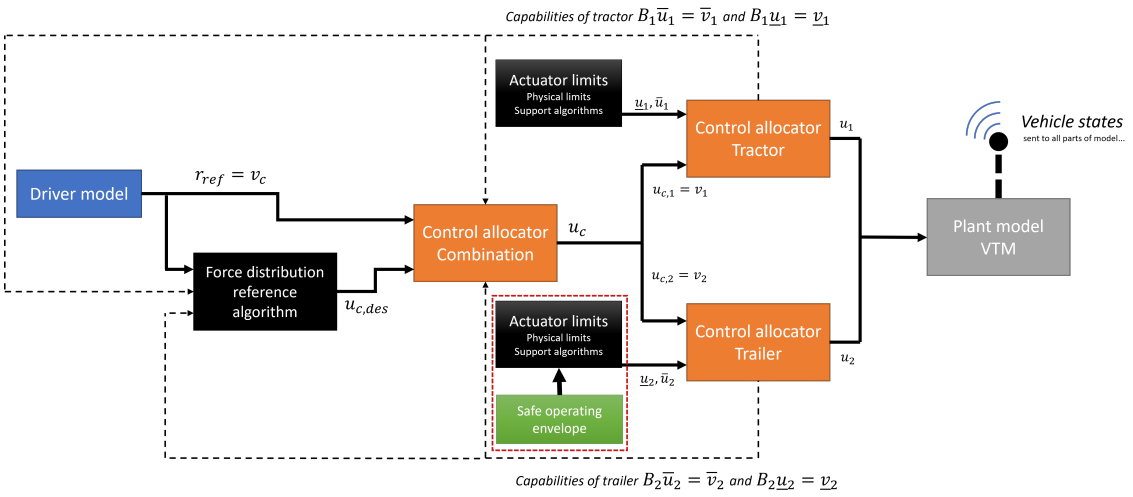

Figure 4.2: Conceptual architecture of control system, including the dynamic selection of $\boldsymbol{u}_{des,c}$

If Algorithm 3 is implemented in the control system, the weight matrix $W_{u,c}$ is set as a 8-by-8 identity matrix as to not disturb the reference set in $\boldsymbol{u}_{des,c}$. If however the algorithm is not used, then $W_{u,c}$ can be set as for instance

$$W_{u,c} = \text{diag}\begin{bmatrix} 1 & 1 & 1 & 0.1 & 1 & 1 & 1 & 0.1 \end{bmatrix} \tag{4.43}$$

where $M_{z_{V,1}}$ and $M_{z_{V,2}}$ are given low weights as to not prioritize the distribution of desired moments around each unit which are the more difficult motions to control on the vehicle.

The scaling parameters in the control allocators are set as the following

$$\gamma_c = 100 \tag{4.44}$$
$$\gamma_1 = 1 \tag{4.45}$$
$$\gamma_2 = 1 \tag{4.46}$$

as to choose an appropriate prioritization between the input signal error and the virtual control signal error.

4.5 Limiting lateral acceleration of tractor

The installed control systems on the vehicle are designed to distribute forces among all actuators on the vehicle in order to fulfill requested global forces. The control systems use actuator limits to determine what available vehicle movement is considered to induce safe driving. However, none of the control systems presented earlier in chapter 4 are predictive and can not limit the motion of the vehicle before a possibly dangerous driving situation may occur. The installed systems can at times react too slow which for instance can make the vehicle steer off track. A common driving scenario where the control systems are slow to react is when the vehicle enter a sharp turn at a high speed. The sudden change in requested lateral force on the vehicle will not be able to be fulfilled and the vehicle will thus skid off track. By monitoring the lateral accelerations of the first axle of the tractor, the vehicle can be sent brake requests as to allow for the control systems to handle the requested global forces and to avoid unsafe driving. If the lateral acceleration of the first axle on the tractor is larger than the slip limit for the wheels, together with a safety factor, as

$$a_{y_{11}} \geq \zeta \mu g \tag{4.47}$$

then the requested longitudinal acceleration on the vehicle is set to $-0.2\frac{m}{s^2}$. ζ is the safety ratio for utilizing the friction limit. This is necessary to allow for the system to react in time and is chosen as 0.5 from experience in simulations.

This solution of controlling the lateral acceleration on the tractor is not general as the brake force is arbitrarily chosen and the safety factor ζ should be replaced with a more sophisticated way of estimating the slip limits of each wheel. For instance, if the slip can be estimated on all wheels of the vehicle then capabilities of each axle of each unit can be quantified and sent to the combination allocator in order to distribute longitudinal and lateral forces of the vehicle without risking unsafe driving. However, as further discussed in chapter 6, this method is sufficient in avoiding unsafe driving for many use cases, some of which are presented in chapter 5.

Algorithm 3 Dynamic selection of $\boldsymbol{u}_{des,c}$

Input: $\underline{\boldsymbol{u}}$,$\overline{\boldsymbol{u}}$,$\boldsymbol{v}_c$,$\boldsymbol{\lambda}$,$\boldsymbol{\kappa}$, n
Output: $\boldsymbol{u}_{des,c}$

$\underline{\boldsymbol{u}} \subseteq \begin{bmatrix} \underline{\boldsymbol{u}}_{em,1} & \underline{\boldsymbol{u}}_{sb,1} & \underline{\boldsymbol{u}}_{em,2} & \underline{\boldsymbol{u}}_{sb,2} & \dots & \underline{\boldsymbol{u}}_{em,n} & \underline{\boldsymbol{u}}_{sb,n} \end{bmatrix}$
$\overline{\boldsymbol{u}} \subseteq \begin{bmatrix} \overline{\boldsymbol{u}}_{em,1} & \overline{\boldsymbol{u}}_{sb,1} & \overline{\boldsymbol{u}}_{em,2} & \overline{\boldsymbol{u}}_{sb,2} & \dots & \overline{\boldsymbol{u}}_{em,n} & \overline{\boldsymbol{u}}_{sb,n} \end{bmatrix}$
$\boldsymbol{v}_c \subseteq \begin{bmatrix} F_{x,req} & F_{y,req} & M_{z,1,req} & M_{z,2,req} & \dots & M_{z,n,req} \end{bmatrix}$
$\boldsymbol{u}_{des,c} \subseteq \begin{bmatrix} F^{des}_{x,em,1} & F^{des}_{x,sb,1} & F^{des}_{y,1} & M^{des}_{z,1} & F^{des}_{x,em,2} & F^{des}_{x,sb,2} & F^{des}_{y,2} & M^{des}_{z,2} & \dots \\ \dots & F^{des}_{x,em,n} & F^{des}_{x,sb,n} & F^{des}_{y,n} & M^{des}_{z,n} \end{bmatrix} = \boldsymbol{0}$

$F_{split,1} \leftarrow \lambda_1 F_{x,req}$
$F_{split,2} \leftarrow \lambda_2 F_{x,req}$
$\vdots$
$F_{split,n} \leftarrow \lambda_n F_{x,req}$
if $F_{x,req} > 0$ **then**
  Split propelling force on units:
  for $j \leftarrow 1$ to n **do**
    $F_{x,rem} = F_{x,req} - \sum \boldsymbol{u}_{des,c}$
    $F^{des}_{x,em,j} = \min(\overline{\boldsymbol{u}}_{em,j}, F_{split,j}, F_{x,rem})$
  end for
else
  Calculate total brake force per unit:
  $F^{tot}_x = \boldsymbol{0}$
  for $j \leftarrow 1$ to n **do**
    $F_{x,rem} = F_{x,req} - \sum F^{tot}_x$
    $F^{tot}_{x,j} = \max(\underline{\boldsymbol{u}}_{em,j} + \underline{\boldsymbol{u}}_{sb,j}, F_{split,j}, F_{x,rem})$
  end for
  Distribute brake forces on em and sb on each unit:
  for $j \leftarrow 1$ to n **do**
    $F^{em}_{split} \leftarrow \kappa_{em} F^{tot}_{x,j}$
    $F^{sb}_{split} \leftarrow \kappa_{sb} F^{tot}_{x,j}$
    $F^{des}_{x,em,j} = \max(\underline{\boldsymbol{u}}_{em,j}, F^{em}_{split}, F^{tot}_{x,j})$
    $F^{des}_{x,sb,j} = \max(\underline{\boldsymbol{u}}_{sb,j}, F^{sb}_{split}, F^{tot}_{x,j} - F^{des}_{x,em,j})$
  end for
end if
$F^{des}_{y,1} \leftarrow F_{y,req}$
$M^{des}_{z,1} \leftarrow M_{z,1,req}$
$M^{des}_{z,2} \leftarrow M_{z,2,req}$
$\vdots$
$M^{des}_{z,n} \leftarrow M_{z,n,req}$

5

Results

This chapter presents the performance of the developed control systems when simulated through different test cases. The two main parts of the control system, i.e. SOE and control allocators, are tested both independently and in conjunction with each other. Test cases include both a standardized ISO test as well as an S-curve turning maneuver. All results are presented in appropriate plots and tables.

5.1 SOE

Two different aspects of the SOE are investigated, function and computational demand. These aspects covers its performance with regards to vehicle motion as well as how execution time changes with the number of points in the envelope.

5.1.1 S-curve

The purpose of the SOE developed in chapter 3 is to limit the total applied torque on the semi-trailer. To verify that the envelope can limit the semi-trailer the vehicle was initiated at an S-curve track consisting of two opposing 90° turns. The curve radius is set to 40 m and the initial speed is 30 km/h. The same vehicle combination as in section 3.2 is used where only the trailer is propelling the vehicle forward. No control allocation or other control systems are enabled. The vehicle is accelerated using the trailer at about 1 $\frac{m}{s^2}$. This is done twice, once with the SOE enabled and once with it disabled. The outcomes of the simulations are shown in Figure 5.1. When the envelope is disabled, jack-knifing occurs and the simulation is terminated. With the envelope enabled the vehicle manages to complete the track without ending up in an unsafe mode. For comparison, a vehicle with only the truck propelling with no control systems installed (similar to a conventional ICE tractor semi-trailer combination) on the same track, the vehicle manages to drive through the entire track.

The total applied trailer torques for the two simulations are shown in Figure 5.2 where it is apparent that the envelope actively limits the upper limits of the torque with a high frequency.

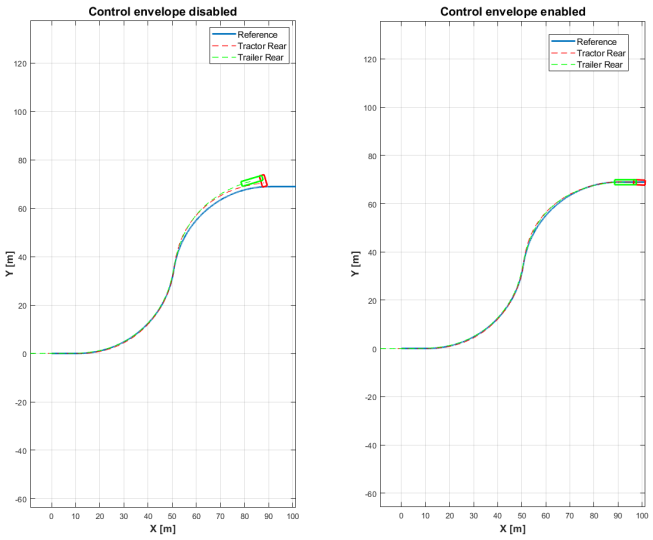

Figure 5.1: Vehicle paths with SOE disabled and enabled

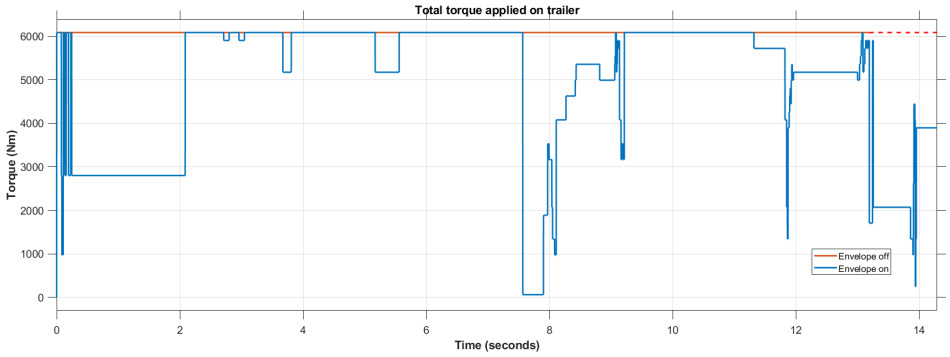

Figure 5.2: Total trailer torque with SOE disabled and enabled

However if the vehicle is initiated at higher speeds or if the radii of the track are decreased then the SOE can not prevent unsafe driving. This is expected and is further discussed in chapter 6.

5.1.2 Execution time

In order to evaluate how computationally demanding the SOE is to use, the execution time of Algorithm 1 is analyzed. This is done by running the algorithm with a set of prerecorded input signals, which originates from a 10 second long simulation. To be able to characterize the computational demand, the envelope is scaled to include different number of data points. All execution times are normalized with regards to the SOE with the least amount of points. Results are presented in Table 5.1.

Table 5.1: Normalized execution time when using differently sized SOEs

Data points in SOE	Execution time (normalized)
5000	1.0000
10000	1.2415
50000	3.8870
100000	4.8889
150000	7.1933
200000	8.3179
250000	8.9916

5.2 Control Allocation

Now the control allocators are enabled in the vehicle together with the SOE and the rest of the control systems. The vehicle is driven in different scenarios and the results of each use case are presented here. Both the tractor and semi-trailer are allowed to propel and brake the vehicle.

5.2.1 S-curve

The same track is used as in section 5.1 and the vehicle is initiated at 30 km/h and is accelerated at about $1\frac{m}{s^2}$. Since the vehicle is accelerating throughout the curve, it will achieve a high enough speed to engage the lateral acceleration control system presented in section 4.5. This will brake the vehicle and thus the chosen driving scenario is considered appropriate since it will include both acceleration and braking of the vehicle while turning. With $\mu = 0.5$ the vehicle manages to get through the track safe and the traveled path of the truck and trailer are shown together with the road reference in Figure 5.3.

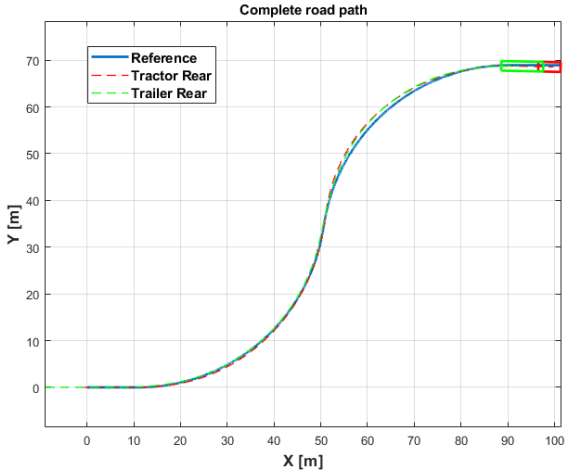

Figure 5.3: Traveled path of vehicle in S-curve

The global forces that are allocated to each unit are shown in Figure 5.4. These forces are distributed among each unit's actuators as depicted in Figures 5.5-5.7.

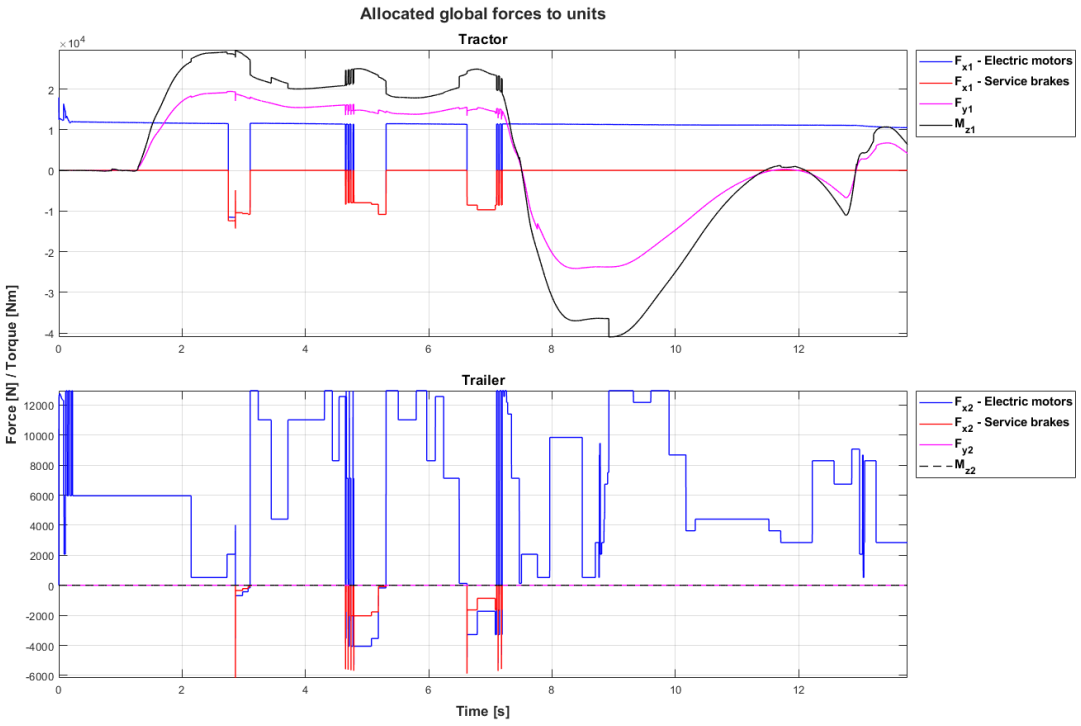

Figure 5.4: Allocated global forces to each unit

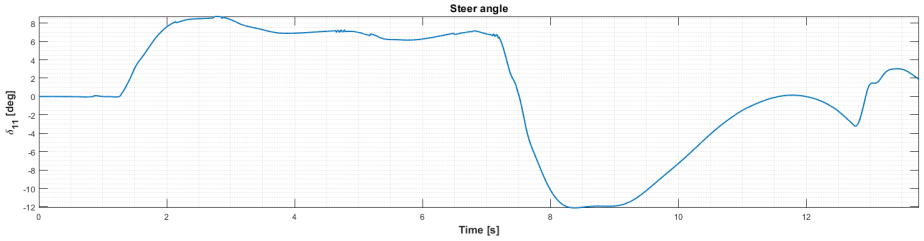

Figure 5.5: Steer angle on first axle of the tractor, δ_{11}

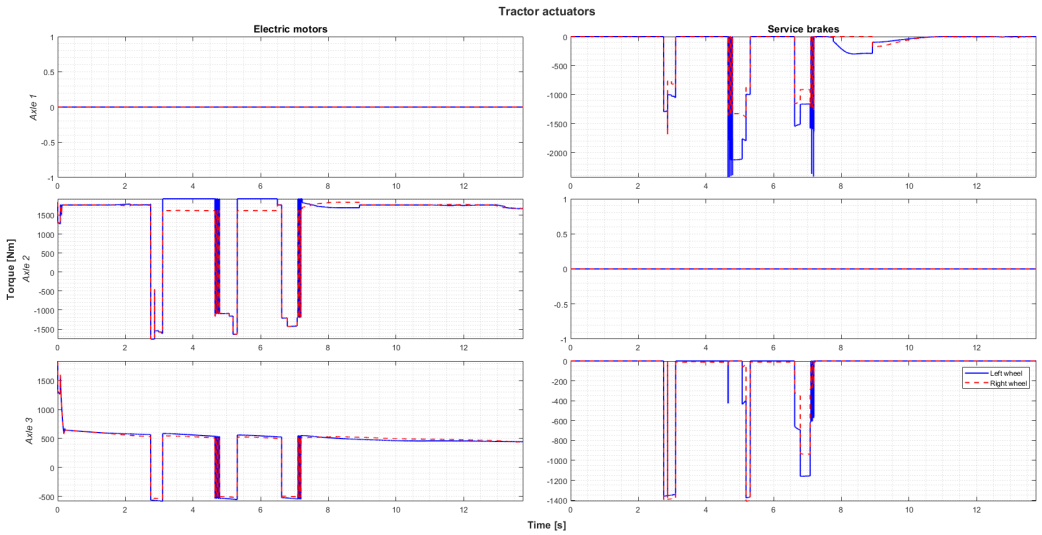

Figure 5.6: Electric motors and service brakes on tractor

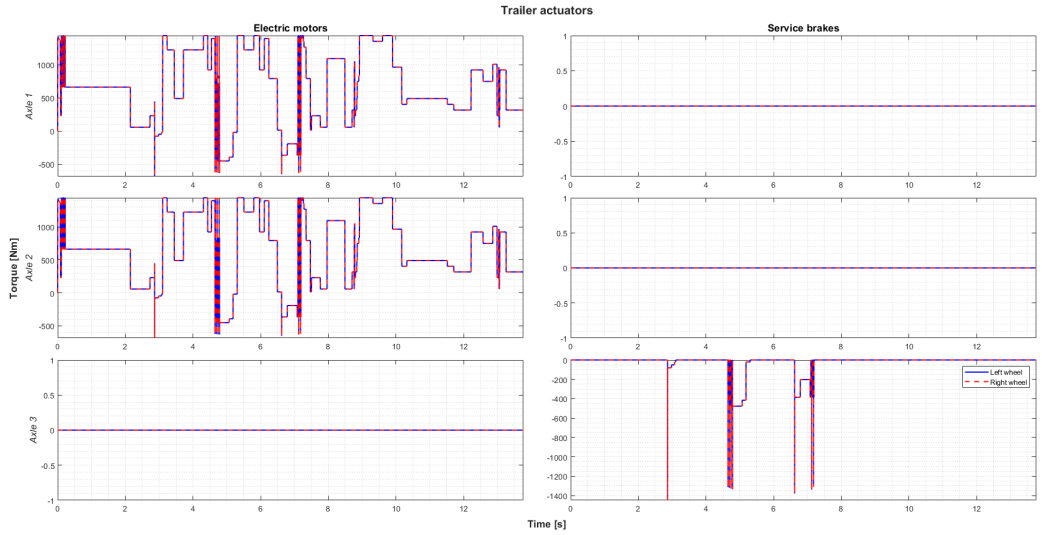

Figure 5.7: Electric motors and service brakes on trailer

5.2.2 Sine with dwell

The International Standard ISO 18375:2016 [30] is a test method for determining the yaw stability of heavy vehicles, including trucks, trailers and buses, on low friction surfaces. The test consist of running a vehicle on a surface with uniform friction coefficient with an initial longitudinal velocity of 50 km/h with the cruise controller activated. A sine with dwell steering input with a frequency of 0.3 Hz and a dwell time of $T_d = 0.75$ s, as depicted in Figure 5.8, is then applied at time T_0.

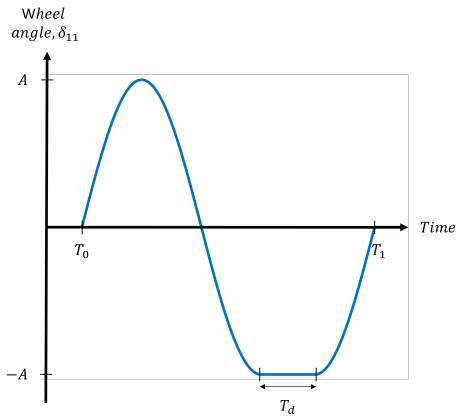

Figure 5.8: Steering input for the sine with dwell test with amplitude A

The yaw stability is evaluated by analyzing characteristic values including for example the yaw stability factor (YSF) over time, maximum articulation angle and final yaw angle. The YSF is defined as

$$YSF_i(t+T_i) = \frac{|\omega_i(t+T_i)|}{|\omega_{i,peak}|}, \tag{5.1}$$

where i denotes the vehicle unit, $\omega_{i,peak}$ is unit i's peak yaw velocity and $\omega_i(t+T_i)$ is the yaw velocity at time $t+T_i$. T_i is the time at which the steering procedure is completed plus the delay in yaw velocity introduced for trailing units. That is, for unit 1, $T_i = T_1$ and for unit 2, $T_i = T_1 + \Delta T$. The YSF characteristic is evaluated at different times $t > 0$ in order to determine whether or not it converges to zero. Fast convergence implies good stability. The maximum articulation angle and the final yaw angle of a vehicle can also be used to determine whether the vehicle enters an unsafe state such as jack-knifing. The yaw stability of a vehicle is evaluated for different steering wheel amplitudes and different surface friction coefficients, where the obtained characteristic values can be used to compare the performance of different vehicles.

In order to conclude how well the developed control system performs, the sine with dwell test is simulated for different tractor semi-trailer setups. These are:

- Vehicle setup 1: Propelling tractor, trailer only equipped with service brakes. Evenly distributed torque on driven wheels of tractor.
- Vehicle setup 2: Both units propelling. Unit and combination level control allocators activated.
- Vehicle setup 3: Both units propelling. Unit and combination level control allocators as well as the SOE activated.
- Vehicle setup 4: Both units propelling. Unit and combination level control allocators activated. SOE and lateral acceleration limiter from section 4.5 enabled.

Table C.1 and C.2 present the resulting characteristics of the sine with dwell simulations for each vehicle setup.

6

Conclusions

The main purpose of the thesis is to investigate whether an e-trailer can be used as a propelling unit in a safe manner in a vehicle combination, consisting of a tractor and a semi-trailer. The purpose is fulfilled by following the objectives set up in section 1.3.

Overall the implemented control strategy of using a torque limiting SOE together with both unit and combination level control allocators allows for the possibility of using the e-trailer for propulsion in a safe manner in many different driving scenarios. However, the proposed systems have some limitations and weaknesses which will be discussed further in this chapter.

6.1 Safe operating envelope

The 6-dimensional SOE used to limit the trailer's applied torque is seen to perform as expected both independently, in section 5.1, as well as in conjunction with the control allocators, in section 5.2. The algorithm reads the state of the vehicle, compares that to the simulated data points and sets torque limits correspondingly. In situations where only the trailer is used for propulsion and the vehicle is driven at an appropriate velocity while entering a curve, the SOE will be sufficient to prevent the vehicle from entering any unsafe state. However, since the system cannot predict the path ahead of the vehicle it will not be able to prevent the vehicle from entering an unsafe state when reaching a sharp curve at high velocity. This is due to the vehicle entering the curve in a state that is unsafe from the beginning, and since the SOE is only designed to maintain the vehicle in a safe state it is not able to recover the vehicle from an already unsafe state. In such cases the vehicle will begin off-tracking. This behavior is, however, not a consequence of implementing the SOE since the same behavior is obtained for any road vehicle facing a high curvature road at high velocity.

When used in conjunction with the control allocators, and thus with a propelling tractor, the SOE also functions as intended. Trailer propulsion is limited in the same way as when using a passive tractor, preventing jack-knifing, trailer swing and roll over. The main difference when using the SOE in a vehicle combination with two propelling units is that the torque can be allocated to the tractor instead of the trailer. This is because the SOE will lower the capability of the trailer, which is sent to the combination level control allocator. In order for the allocator to fulfill

the driver requests more propulsion force will then be allocated to the tractor. This behavior can increase the velocity of the vehicle which in turn can cause off-tracking. Because of this the lateral acceleration limiter, described in section 4.5, or a similar controller that limits slip on the front most axle is essential when using a SOE in a vehicle combination where both units are propelling.

Another important factor to consider is how computationally demanding the SOE will be when run in a real vehicle. The envelope needs to have sufficient resolution to cover as many states of the vehicle as possible, but at the same time the run-time of the algorithm increases with the number of data points. The SOE containing 393600 data points drastically slows down the system and it is possible to ensure safe vehicle motion by using fewer data points. Fewer data points can however result in a more restrictively propelling trailer since the SOE will contain data corresponding to fewer states. This means that the closest safe point is more likely to deviate from the current state of the vehicle. The closest safe point always correspond to an equally or more difficult driving scenario (for instance smaller μ, larger v_x or larger θ) and if the point deviates significantly from the current vehicle state the outputted maximum applicable trailer torque can be more restrained than it needs to be.

6.2 Control system

The S-curve and the sine with dwell proved to be sufficiently difficult and versatile enough test cases to draw conclusions about the performance of the proposed control systems. Both strengths and weaknesses of the systems were exposed and further improvements are shown to be needed to make the vehicle handle a wider range of driving scenarios.

6.2.1 S-curve

The control systems implemented managed to safely make the vehicle travel through the S-curve test track with some limitations. When the vehicle was initiated on the track at too high speeds the control systems could not predict that the upcoming sharp turn would induce unsafe driving. This often resulted in the vehicle off-tracking. However when the speed was low enough, the systems managed to control the vehicle in a safe and energy efficient way.

The combination control allocation distributed global forces well and it is apparent from Figure 5.4 when the driver requests the vehicle to accelerate, brake or steer. It also recognizes the capabilities of each unit and distributes forces accordingly. The unit level control allocators uses the actuators to a minimum and no actuators are working against each other unnecessarily while completing the desired movements requested by the combination level allocator. Also, when braking the forces are distributed as expected using brake blending (from subsection 4.3.3). The steer angle is affected only slightly by the steering support system but it helps to increase the capabilities in $F_{y_{V,1}}$ and $M_{z_{V,1}}$.

6.2.2 Yaw stability of vehicle

When implementing additional functionality contributing to vehicle motion it is important to make sure that the vehicle maintains good yaw stability. The characteristic values of the sine with dwell tests, as performed in subsection 5.2.2, show that the complete control system is able to perform equally well as a traditional pulling tractor and passive semi-trailer combination, from a yaw stability standpoint. For $\mu = 0.5$, the traditional tractor semi-trailer combination is able to handle a wheel angle of $\delta_{11} = 10.5°$ before facing severe instability. When instead using an e-trailer and the complete control system, the YSF values of both units do not converge towards zero which implies instability. However, the system is stable at the slightly lower angle $\delta_{11} = 10°$. This small difference in performance is deemed negligible.

For the lower friction coefficient $\mu = 0.3$ both the traditional tractor semi-trailer combination and the combination with an e-trailer and dedicated control system manages to handle steering angles of up to $\delta_{11} = 12.5°$. Based on the maximum yaw velocity of the vehicle, larger steering angles can likely not be handled due to under steering. A larger steering angle will result in a larger maximum yaw velocity as long as the vehicle maintains traction, which is not the case in Table C.2. However, the e-trailer combination is seen to end up in an unsafe mode using vehicle setup 2 and 3, whereas vehicle setup 4 matches the stability of the traditional truck.

The results for both friction coefficients declares that using only control allocators or control allocators in conjunction with the SOE is not enough to ensure safe vehicle motion. The results also reveals that the SOE does not improve the yaw stability for this kind of driving scenario. This is likely because of the same reason as discussed in section 6.1, where the vehicle enters the steering procedure at high velocity and thus enters an unsafe state before the SOE is able to limit the system. By also adding the lateral acceleration limiter the vehicle obtains similar performance as the traditional vehicle combination, which implies that it is possible to use the control system for safe vehicle motion in a two unit-propelled vehicle combination.

6.2.3 Tuning and performance

The S-curve and sine with dwell test cases worked well with the selected tuning parameters of the control allocators and driver model. However the performance and behavior of the vehicle is greatly affected by these choices and different values of these parameters can completely change the outcome of each simulation. As the chosen scenarios and the objective of the thesis is to safely propel an electric tractor semi-trailer in an energy-efficient way, the choice of tuning parameters in the control allocators are made in such a way as to minimize actuator usage and to avoid actuators and the two units to counteract each other. The choices of γ, W_v and W_u in each allocator does not favor achieving the requested global forces (which in terms of optimization means minimizing $B\boldsymbol{u} - \boldsymbol{v}$). Using the selected control system in other driving scenarios does therefore not always guarantee safe driving of the vehicle.

The driver model used to simulate a real driver following a road with a set speed also contain many tuning parameters which can be chosen to favor different use cases. These parameters are tuned to fit the chosen test scenarios well and to mimic a real life driver. However other scenarios may need different tuning of the driver model. The results were determined to not have been biased by the driver model since it was also determined that an experienced real life driver would perform better than the driver model regarding path following and speed control which in turn would help the vehicle drive better.

It was apparent when using a simplified tire model in the B-matrices and translation of driver input, the choice of the cornering stiffness C_{11} had a large effect on the performance of the system. The cornering stiffness must be approximated for different driving scenarios and would ideally be chosen based on tire properties and environment parameters. However, as with the driver model, it was determined that the choice of C_{11} was suitable and did not introduce a positive bias to the simulation results even though it not being suitable for other, different driving scenarios.

6.3 Future work

The objectives of the thesis are satisfied with fair results. However there are many improvements that can be done to the found solutions to improve the quality of the results. These improvements were not done in the thesis due to the limited time frame and labor force.

To reduce the development time when testing the control systems and in particular the SOE, the developed envelope algorithm can be optimized to further increase the computational speed of the system when simulating. Using more sophisticated algorithms, using a neural network or using machine learning could reduce the computational time and thus allow for faster development of the system.

The implemented control systems should be complemented with predictive control as to allow for a wider range of driving scenarios. Tuning parameters in control allocators could be chosen dynamically using advanced algorithms as to also cover more driving scenarios without the need of tuning the control system for every unique scenario and drive style. Also, since a simplified tire model is used when estimating the lateral tire forces, the choice of C_{11} can also be done dynamically which could improve the performance of the vehicle.

Energy effectiveness has been a part in the development in this thesis. However no measures of for instance the range of the vehicle has been made. The actual range of the vehicle with different control strategies could be measured as to quantify how energy efficient the applied vehicle system actually is.

Bibliography

[1] H. Ritchie and M. Roser, "CO2 and Greenhouse Gas Emissions," *Our World in Data*, 2020. [Online]. Available: https://ourworldindata.org/co2-and-other-greenhouse-gas-emissions (visited on 01/28/2022).

[2] I. Tieso. "Road freight fleet emissions worldwide as of 2020, by vehicle type." (Jan. 2022), [Online]. Available: https://www.statista.com/statistics/1200116/road-freight-emissions-by-vehicle-type-worldwide/ (visited on 01/28/2022).

[3] S. Downing. "8 electric truck and van companies to watch in 2020." (Jan. 2020), [Online]. Available: https://www.greenbiz.com/article/8-electric-truck-and-van-companies-watch-2020 (visited on 01/28/2022).

[4] Volvo Trucks. "Switch to electric." (Apr. 2021), [Online]. Available: https://brochures.volvotrucks.com/hq/electromobility/switch-to-electric-master-en/?page=1 (visited on 04/26/2022).

[5] E. Commission. "Driving time and rest periods in the road transport sector." (Nov. 2020), [Online]. Available: https://eur-lex.europa.eu/summary/EN/legissum:c00018 (visited on 05/30/2022).

[6] S. O. Hansson, M.-Å. Belin, and B. Lundgren, "Self-driving vehicles—an ethical overview," *Philosophy & Technology*, vol. 34, Dec. 2021. DOI: 10.1007/s13347-021-00464-5.

[7] United Nations, Department of Economic and Social Affairs. "The 17 goals | sustainable development." (2022), [Online]. Available: https://sdgs.un.org/goals (visited on 04/27/2022).

[8] Volvo 3P, "VTM Plant Model Description," Unpublished internal company document, 2018.

[9] P. Sundström and L. Laine, "Validation of vtm model of tractor 4x2 with semi-trailer using winter test results from arjeplog 2111w11 p2685," *Engineering Report ER-624557, Department of Applied Mechanics, Chalmers University of Technology*, 2012.

[10] B. Westerhof and D. Kalakos, "Heavy vehicle braking using friction estimation for controller optimization," M.S. thesis, 2017.

[11] H. Pacejka, *Tire and vehicle dynamics*. Elsevier, 2005.

[12] International Organization for Standardization, *Road vehicles – Vehicle dynamics and road-holding ability – Vocabulary*, ISO 8855:2011(E). Geneva, Switzerland: International Organization for Standardization, 2011. [Online]. Available: https://www.iso.org/standard/51180.html.

[13] S. Sun and C. C. de Visser, "Quadrotor Safe Flight Envelope Prediction in the High-Speed Regime: A Monte-Carlo Approach," in *AIAA Scitech 2019 Forum*, Reston, Virginia: American Institute of Aeronautics and Astronautics, Jan. 2019, pp. 1–12, ISBN: 978-1-62410-578-4. DOI: 10.2514/6.2019-0948. [Online]. Available: https://arc.aiaa.org/doi/10.2514/6.2019-0948.

[14] R. van den Brandt and C. de Visser, "Safe flight envelope uncertainty quantification using probabilistic reachability analysis," *IFAC-PapersOnLine*, vol. 51, no. 24, pp. 628–635, 2018, 10th IFAC Symposium on Fault Detection, Supervision and Safety for Technical Processes SAFEPROCESS 2018, ISSN: 2405-8963. DOI: https://doi.org/10.1016/j.ifacol.2018.09.641. [Online]. Available: https://www.sciencedirect.com/science/article/pii/S240589631832353X.

[15] C. E. Beal and J. C. Gerdes, "Model predictive control for vehicle stabilization at the limits of handling," *IEEE Transactions on Control Systems Technology*, vol. 21, no. 4, pp. 1258–1269, 2013. DOI: 10.1109/TCST.2012.2200826.

[16] S. M. Erlien, J. Funke, and J. C. Gerdes, "Incorporating non-linear tire dynamics into a convex approach to shared steering control," in *2014 American Control Conference*, 2014, pp. 3468–3473. DOI: 10.1109/ACC.2014.6859116.

[17] S. M. Erlien, S. Fujita, and J. C. Gerdes, "Shared steering control using safe envelopes for obstacle avoidance and vehicle stability," *IEEE Transactions on Intelligent Transportation Systems*, vol. 17, no. 2, pp. 441–451, 2016. DOI: 10.1109/TITS.2015.2453404.

[18] Trafikverket, "Krav för vägars och gators utformning," 2015. [Online]. Available: https://trafikverket.ineko.se/Files/sv-SE/12046/RelatedFiles/2015_086_krav_for_vagars_och_gators_utformning.pdf (visited on 03/16/2022).

[19] E. Commission. "Going abroad - sweden, speed limits." (Apr. 2016), [Online]. Available: https://ec.europa.eu/transport/road_safety/going_abroad/sweden/speed_limits_en.htm (visited on 03/16/2022).

[20] J. Wang and R. G. Longoria, "Coordinated and reconfigurable vehicle dynamics control," *IEEE Transactions on Control Systems Technology*, vol. 17, no. 3, pp. 723–732, 2009. DOI: 10.1109/TCST.2008.2002264.

[21] E. B. Roger, "Application of control allocation methods to linear systems with four or more objectives," Ph.D. dissertation, Virginia Polytechnic Institute and State University, Blacksburg, Va, USA, 2002.

[22] B.-M. Min, E.-T. Kim, and M.-J. Tahk, "Application of control allocation methods to sat-ii uav," Aug. 2005, ISBN: 978-1-62410-056-7. DOI: 10.2514/6.2005-6411.

[23] J. Plumlee, D. Bevly, and A. Hodel, "Control of a ground vehicle using quadratic programming based control allocation techniques," in *Proceedings of the 2004 American Control Conference*, vol. 5, 2004, 4704–4709 vol.5. DOI: 10.23919/ACC.2004.1384055.

[24] K. Tagesson, P. Sundstrom, L. Laine, and N. Dela, "Real-time performance of control allocation for actuator coordination in heavy vehicles," in *2009 IEEE Intelligent Vehicles Symposium*, 2009, pp. 685–690. DOI: 10.1109/IVS.2009.5164359.

[25] B. Källstrand, "Control allocation for vehicle motion control," M.S. thesis, Chalmers University of Technology, Gothenburg, Sweden, Aug. 2016.

[26] O. Härkegård, "Backstepping and control allocation with applications to flight control," Ph.D. dissertation, Linköping University, Linköping, Sweden, Apr. 2003.

[27] J. Eklöv, "Real-time implementation of a vehicle motion coordinator for a single unit truck," Master's Thesis EX036/2013, Chalmers University of Technology, 2013.

[28] P. Nyman and K. Uhlén, "Coordination of actuators for long heavy vehicle combinations using control allocation," M.S. thesis, Chalmers University of Technology, Gothenburg, Sweden, Jun. 2014.

[29] M. Boerboom, "Electric vehicle blended braking maximizing energy recovery while maintaining vehicle stability and maneuverability.," M.S. thesis, 2012.

[30] International Organization for Standardization, *Heavy commercial vehicles and buses – Test method for yaw stability – Sine with dwell test*, ISO 18375:2016. Geneva, Switzerland: International Organization for Standardization, 2016. [Online]. Available: `https://www.iso.org/standard/62291.html`.

A

Mathematical derivations

To derive the B-matrix used in the control allocator for a tractor combined with a three axle semi-trailer as seen in Figure 1.2, equations of motion must be defined. Using Figure 2.4 and 2.3 and assigning $i = 1$ to the tractor and $i = 2$ for the semi-trailer, all forces can be obtained on the vehicle. Since there are only two units in the vehicle, only one coupling force will exist and indices for the articulation angle θ will be omitted. Also, only the first axle of the first unit will be steerable which is why all steering angles except δ_{11} will be equal to zero and are thus omitted from all further calculations.

A.1 B-matrix on combination level

First, the rear coupling forces on the first unit is related to the front coupling forces on the second unit as:

$$F_{xcr_1} = \quad F_{xcf_2}\cos\theta_1 + F_{ycf_2}\sin\theta_1 \tag{A.1}$$
$$F_{ycr_1} = -F_{xcf_2}\sin\theta_1 + F_{ycf_2}\cos\theta_1 \tag{A.2}$$

For clarification, the front coupling forces of the second unit are related to the rear coupling forces of the first unit as:

$$F_{xcf_2} = F_{xcr_1}\cos\theta_1 - F_{ycr_1}\sin\theta_1 \tag{A.3}$$
$$F_{ycf_2} = F_{xcr_1}\sin\theta_1 + F_{ycr_1}\cos\theta_1 \tag{A.4}$$

Using Newtons second laws of motion the following equations of motion of the two units are set up:

$$F_{x,1} = m_1 a_{x_1} = F_{x_{V,1,em}} + F_{x_{V,1,sb}} - F_{xcr_1} - F_{res,1} \tag{A.5}$$
$$F_{y,1} = m_1 a_{y_1} = F_{y_{V,1}} - F_{ycr_1} \tag{A.6}$$
$$M_{z,1} = J_1\dot{\omega}_{z_1} = M_{z_{V,1}} + F_{ycr_1} d_{r_1} \tag{A.7}$$

$$F_{x,2} = m_2 a_{x_2} = F_{x_{V,2,em}} + F_{x_{V,2,sb}} + F_{xcf_2} - F_{res,2} \tag{A.8}$$
$$F_{y,2} = m_2 a_{y_2} = F_{y_{V,2}} + F_{ycf_2} \tag{A.9}$$
$$M_{z,2} = J_2\dot{\omega}_{z_2} = M_{z_{V,2}} + F_{ycf_2} d_{f_2} \tag{A.10}$$

Substituting the coupling forces in A.1 and A.2 with A.8 and A.9 gives:

$$F_{xcr_1} = (m_2 a_{x_2} - F_{x_{V,2,em}} - F_{x_{V,2,sb}} + F_{res,2})\cos\theta_1 + (m_2 a_{y_2} - F_{y_{V,2}})\sin\theta_1 \quad \text{(A.11)}$$
$$F_{ycr_1} = -(m_2 a_{x_2} - F_{x_{V,2,em}} - F_{x_{V,2,sb}} + F_{res,2})\sin\theta_1 + (m_2 a_{y_2} - F_{y_{V,2}})\cos\theta_1 \quad \text{(A.12)}$$

The acceleration on the second unit are expressed in terms of the first unit as:

$$a_{x_2} = a_{x_1}\cos\theta_1 - (a_{y_1} - d_{r_1}\dot{\omega}_{z_1})\sin\theta_1 \quad \text{(A.13)}$$
$$a_{y_2} = a_{x_1}\sin\theta_1 + (a_{y_1} - d_{r_1}\dot{\omega}_{z_1})\cos\theta_1 + d_{f_2}(\ddot{\theta}_1 - \dot{\omega}_{z_1}) \quad \text{(A.14)}$$

The virtual signals for the combination control allocator in Equation 4.7 are expressed using the equations of motion in Equations A.5-A.10. $F_{x,req}$, $F_{y,req}$ are expressed as forces in the coordinate frame of the first unit:

$$F_{x,req} = m_1 a_{x_1} + m_2 a_{x_2}\cos\theta_1 - m_2 a_{y_2}\sin\theta_1 = F_{x_1} + F_{x_2}\cos\theta_1 - F_{y_2}\sin\theta_1 \quad \text{(A.15)}$$
$$F_{y,req} = m_1 a_{y_1} + m_2 a_{y_2}\cos\theta_1 + m_2 a_{x_2}\sin\theta_1 = F_{y_1} + F_{y_2}\cos\theta_1 + F_{x_2}\sin\theta_1 \quad \text{(A.16)}$$
$$M_{z,1,req} = J_1\dot{\omega}_{z_1} = M_{z_{V,1}} + F_{ycr_1} d_{r_1} \quad \text{(A.17)}$$
$$M_{z,2,req} = J_2\dot{\omega}_{z_2} = M_{zt_2} - F_{xcr_1}\sin\theta_1 d_{f_2} - F_{ycr_1}\cos\theta_1 d_{f_2} \quad \text{(A.18)}$$

Substituting all known variables in Equations A.15-A.18 and simplifying using a symbolic calculations tool and moving all variables in $\boldsymbol{u}_c$ and the resistance forces to the right hand side:

$$\begin{bmatrix} F_{x,req} \\ F_{y,req} \\ M_{z,1,req} \\ M_{z,2,req} \end{bmatrix} = \left[\begin{array}{cccc} m_1+m_2 & 0 & -m_2 d_{f_2}\sin\theta_1 & m_2 d_{f_2}\sin\theta_1 \\ \hdashline 0 & m_1+m_2 & -m_2(d_{r_1}+d_{f_2}\cos\theta_1) & m_2 d_{f_2}\cos\theta_1 \\ \hdashline 0 & -m_2 d_{r_1} & -J_1 + m_2 d_{r_1}^2 + m_2 d_{r_1} d_{f_2}\cos\theta_1 & -m_2 d_{r_1} d_{f_2}\cos\theta_1 \\ \hdashline m_2\sin\theta_1 d_{f_2} & m_2\cos\theta_1 d_{f_2} & -J_2 - m_2 d_{f_2}^2 - m_2 d_{r_1} d_{f_2}\cos\theta_1 & J_2 + m_2 d_{f_2}^2 \end{array}\right] \begin{bmatrix} a_{x_1} \\ a_{y_1} \\ \dot{\omega}_{z_1} \\ \ddot{\theta}_1 \end{bmatrix}$$

$$= \begin{bmatrix} -F_{res,1} - F_{res,2}\cos\theta_1 \\ F_{res,2}\sin\theta_1 \\ -F_{res,2}\sin\theta_1 d_{r_1} \\ 0 \end{bmatrix} + \underbrace{\begin{bmatrix} 1 & 1 & 0 & 0 & \cos\theta_1 & \cos\theta_1 & \sin\theta_1 & 0 \\ 0 & 0 & 1 & 0 & -\sin\theta_1 & -\sin\theta_1 & \cos\theta_1 & 0 \\ 0 & 0 & 0 & 1 & d_{r_1}\sin\theta_1 & d_{r_1}\sin\theta_1 & -d_{r_1}\cos\theta_1 & 0 \\ 0 & 0 & 0 & 0 & 0 & 0 & d_{f_2} & 1 \end{bmatrix}}_{B_c} \begin{bmatrix} F_{x_{V,1,em}} \\ F_{x_{V,1,sb}} \\ F_{y_{V,1}} \\ M_{z_{V,1}} \\ F_{x_{V,2,em}} \\ F_{x_{V,2,sb}} \\ F_{y_{V,2}} \\ M_{z_{V,2}} \end{bmatrix}$$

A.2 B-matrix on unit level - Tractor

From Figure 2.4, the virtual control signal $\boldsymbol{v}_{tractor}$ can be expressed using the torques applied on the unit by the actuators and the steering angle of the first axle:

$$
\begin{aligned}
F_{x_{V,1,em}} &= (\frac{T_{11R,em}}{r_1} + \frac{T_{11L,em}}{r_1})\cos(\delta_{11}) - (2C_{11}\delta_{11})\sin(\delta_{11}) + \frac{T_{12R,em}}{r_1} + \frac{T_{12L,em}}{r_1} + \frac{T_{13R,em}}{r_1} + \frac{T_{13L,em}}{r_1} \\
F_{x_{V,1,sb}} &= (\frac{T_{11R,sb}}{r_1} + \frac{T_{11L,sb}}{r_1})\cos(\delta_{11}) + \frac{T_{12R,sb}}{r_1} + \frac{T_{12L,sb}}{r_1} + \frac{T_{13R,sb}}{r_1} + \frac{T_{13L,sb}}{r_1} \\
F_{y_{V,1}} &= (\frac{T_{11R,em}}{r_1} + \frac{T_{11L,em}}{r_1} + \frac{T_{11R,sb}}{r_1} + \frac{T_{11L,sb}}{r_1})\sin(\delta_{11}) + (2C_{11}\delta_{11})\cos(\delta_{11}) + F_{y_{12L}} + F_{y_{12R}} \\
&\quad + F_{y_{13L}} + F_{y_{13R}} \\
M_{z_{V,1}} &= ((\frac{T_{11R,em}}{r_1} + \frac{T_{11R,sb}}{r_1})\cos\delta_{11} - (C_{11}\delta_{11})\sin\delta_{11} - (\frac{T_{11L,em}}{r_1} + \frac{T_{11L,sb}}{r_1})\cos\delta_{11} + (C_{11}\delta_{11})\sin\delta_{11})w_1 \\
&\quad + (\frac{T_{12R,em}}{r_1} + \frac{T_{13R,em}}{r_1} - \frac{T_{12L,em}}{r_1} - \frac{T_{13L,em}}{r_1} + \frac{T_{12R,sb}}{r_1} + \frac{T_{13R,sb}}{r_1} - \frac{T_{12L,sb}}{r_1} - \frac{T_{13L,sb}}{r_1})w_1 \\
&\quad + (C_{11}\delta_{11}\cos\delta_{11} + (\frac{T_{11R,em}}{r_1} + \frac{T_{11R,sb}}{r_1})\sin\delta_{11} + (C_{11}\delta_{11})\cos\delta_{11} + (\frac{T_{11L,em}}{r_1} + \frac{T_{11L,sb}}{r_1})\sin\delta_{11})l_{a,11} \\
&\quad - \underbrace{(F_{y_{12R}} + F_{y_{12L}})}_{0} l_{a,12} - \underbrace{(F_{y_{13L}} + F_{y_{13R}})}_{0} l_{a,13}
\end{aligned}
$$

Here, as in described in Section 4.2.1, a simplified tire model is used where the lateral forces on the tires are linearly proportional to the steering angle. The lateral force on each of the wheels on the first axle is

$$F_{y_{11R}} = F_{y_{11L}} = C_{11}\delta_{11} \tag{A.19}$$

The equations can be split up as $\boldsymbol{v}_c = B_1\boldsymbol{u}_1$:

$$
\begin{bmatrix} F_{x_{V,1,em}} \\ F_{x_{V,1,sb}} \\ F_{y_{V,1}} \\ M_{z_{V,1}} \end{bmatrix} = \begin{bmatrix} \frac{\cos(\delta_{11})}{r_1} & \frac{\cos(\delta_{11})}{r_1} & \frac{1}{r_1} & \frac{1}{r_1} & \frac{1}{r_1} & \frac{1}{r_1} & \dots \\ 0 & 0 & 0 & 0 & 0 & 0 & \dots \\ \frac{\sin(\delta_{11})}{r_1} & \frac{\sin(\delta_{11})}{r_1} & 0 & 0 & 0 & 0 & \dots \\ \frac{l_{a,11}\sin(\delta_{11})}{r_1} - \frac{w_{11}\cos(\delta_{11})}{r_1} & \frac{w_{11}\cos(\delta_{11})}{r_1} + \frac{l_{a,11}\sin(\delta_{11})}{r_1} & -\frac{w_{12}}{r_1} & \frac{r_1}{r_1} & -\frac{w_{13}}{r_1} & \frac{w_{13}}{r_1} & \dots \end{bmatrix}
$$

$$
\begin{bmatrix} 0 & 0 & 0 & 0 & 0 & 0 & -2\,\mathrm{C}_{11}\,\sin(\delta_{11}) \\ \frac{\cos(\delta_{11})}{r_1} & \frac{\cos(\delta_{11})}{r_1} & \frac{1}{r_1} & \frac{1}{r_1} & \frac{1}{r_1} & \frac{1}{r_1} & 0 \\ \frac{\sin(\delta_{11})}{r_1} & \frac{\sin(\delta_{11})}{r_1} & 0 & 0 & 0 & 0 & 2\,\mathrm{C}_{11}\,\cos(\delta_{11}) \\ \frac{l_{a,11}\sin(\delta_{11})}{r_1} - \frac{w_{11}\cos(\delta_{11})}{r_1} & \frac{w_{11}\cos(\delta_{11})}{r_1} + \frac{l_{a,11}\sin(\delta_{11})}{r_1} & -\frac{w_{12}}{r_1} & \frac{w_{12}}{r_1} & -\frac{w_{13}}{r_1} & \frac{w_{13}}{r_1} & 2\,\mathrm{C}_{11}\,l_{a,11}\,\cos(\delta_{11}) \end{bmatrix}
\begin{bmatrix} T_{11L,em} \\ T_{11R,em} \\ T_{12L,em} \\ T_{12R,em} \\ T_{13L,em} \\ T_{13R,em} \\ T_{11L,sb} \\ T_{11R,sb} \\ T_{12L,sb} \\ T_{12R,sb} \\ T_{13L,sb} \\ T_{13R,sb} \\ \delta_{11} \end{bmatrix}
$$

As explained in section 4.2.1 it is desired for Equation 4.11 to correspond with the last column in the B-matrix above. This is possible if the column is linearized around

$\delta_{11} = 0$ which will result in the following B-matrix for the tractor unit:

$$B_1 = \begin{bmatrix} \frac{\cos(\delta_{11})}{r_1} & \frac{\cos(\delta_{11})}{r_1} & \frac{1}{r_1} & \frac{1}{r_1} & \frac{1}{r_1} & \frac{1}{r_1} & \dots \\ 0 & 0 & 0 & 0 & 0 & 0 & \dots \\ \frac{\sin(\delta_{11})}{r_1} & \frac{\sin(\delta_{11})}{r_1} & 0 & 0 & 0 & 0 & \dots \\ \frac{l_{a,11}\,\sin(\delta_{11})}{r_1} - \frac{w_{11}\,\cos(\delta_{11})}{r_1} & \frac{w_{11}\,\cos(\delta_{11})}{r_1} + \frac{l_{a,11}\,\sin(\delta_{11})}{r_1} & -\frac{w_{12}}{r_1} & \frac{w_{12}}{r_1} & -\frac{w_{13}}{r_1} & \frac{w_{13}}{r_1} & \dots \end{bmatrix}$$

$$\begin{bmatrix} 0 & 0 & 0 & 0 & 0 & 0 & 0 \\ \frac{\cos(\delta_{11})}{r_1} & \frac{\cos(\delta_{11})}{r_1} & \frac{1}{r_1} & \frac{1}{r_1} & \frac{1}{r_1} & \frac{1}{r_1} & 0 \\ \frac{\sin(\delta_{11})}{r_1} & \frac{\sin(\delta_{11})}{r_1} & 0 & 0 & 0 & 0 & 2\,\mathrm{C}_{11} \\ \frac{l_{a,11}\,\sin(\delta_{11})}{r_1} - \frac{w_{11}\,\cos(\delta_{11})}{r_1} & \frac{w_{11}\,\cos(\delta_{11})}{r_1} + \frac{l_{a,11}\,\sin(\delta_{11})}{r_1} & -\frac{w_{12}}{r_1} & \frac{w_{12}}{r_1} & -\frac{w_{13}}{r_1} & \frac{w_{13}}{r_1} & 2\,\mathrm{C}_{11}\,l_{a,11} \end{bmatrix}$$

A.3 B-matrix on unit level - Trailer

Similarly as in Appendix A.2, the equations for the trailer unit is defined as follows:

$$\begin{aligned} F_{x_{V,2,em}} &= \frac{T_{21R,em}}{r_2} + \frac{T_{21L,em}}{r_2} + \frac{T_{22R,em}}{r_2} + \frac{T_{22L,em}}{r_2} + \frac{T_{23R,em}}{r_2} + \frac{T_{23L,em}}{r_2} \\ F_{x_{V,2,sb}} &= \frac{T_{21R,sb}}{r_2} + \frac{T_{21L,sb}}{r_2} + \frac{T_{22R,sb}}{r_2} + \frac{T_{22L,sb}}{r_2} + \frac{T_{23R,sb}}{r_2} + \frac{T_{23L,sb}}{r_2} \\ F_{y_{V,2}} &= 0 \\ M_{z_{V,2}} &= (\frac{T_{21R,em}}{r_2} - \frac{T_{21L,em}}{r_2} + \frac{T_{22R,em}}{r_2} - \frac{T_{22L,em}}{r_2} + \frac{T_{23R,em}}{r_2} - \frac{T_{23L,em}}{r_2} \\ &\quad + \frac{T_{21R,sb}}{r_2} - \frac{T_{21L,sb}}{r_2} + \frac{T_{22R,sb}}{r_2} - \frac{T_{22L,sb}}{r_2} + \frac{T_{23R,sb}}{r_2} - \frac{T_{23L,sb}}{r_2})w_2 \end{aligned}$$

The equations are split up as $\boldsymbol{v}_2 = B_2\boldsymbol{u}_2$:

$$\begin{bmatrix} F_{x_{V,2,em}} \\ F_{x_{V,2,sb}} \\ F_{y_{V,2}} \\ M_{z_{V,2}} \end{bmatrix} = \underbrace{\begin{bmatrix} \frac{1}{r_2} & \frac{1}{r_2} & \frac{1}{r_2} & \frac{1}{r_2} & \frac{1}{r_2} & \frac{1}{r_2} & 0 & 0 & 0 & 0 & 0 & 0 \\ 0 & 0 & 0 & 0 & 0 & 0 & \frac{1}{r_2} & \frac{1}{r_2} & \frac{1}{r_2} & \frac{1}{r_2} & \frac{1}{r_2} & \frac{1}{r_2} \\ 0 & 0 & 0 & 0 & 0 & 0 & 0 & 0 & 0 & 0 & 0 & 0 \\ -\frac{w_{21}}{r_2} & \frac{w_{21}}{r_2} & -\frac{w_{22}}{r_2} & \frac{w_{22}}{r_2} & -\frac{w_{23}}{r_2} & \frac{w_{23}}{r_2} & -\frac{w_{21}}{r_2} & \frac{w_{21}}{r_2} & -\frac{w_{22}}{r_2} & \frac{w_{22}}{r_2} & -\frac{w_{23}}{r_2} & \frac{w_{23}}{r_2} \end{bmatrix}}_{B_2} \begin{bmatrix} T_{21L,em} \\ T_{21R,em} \\ T_{22L,em} \\ T_{22R,em} \\ T_{23L,em} \\ T_{23R,em} \\ T_{21L,sb} \\ T_{21R,sb} \\ T_{22L,sb} \\ T_{22R,sb} \\ T_{23L,sb} \\ T_{23R,sb} \end{bmatrix}$$

B

Vehicle specifications

The presented specifications for the tractor semi-trailer vehicle combination throughout the thesis are based on the vehicle parameters sheets from "ReVeRe 6x4 tractor A-786343" and "Semitrailer SEM 219" and are presented in Table B.1:

Table B.1: Vehicle parameters

Unit	1			2		
Axle	1	2	3	1	2	3
Axle loads (m) [kg]	6765.5	3654.8	3654.8	2641.8	2641.8	2641.8
Wheel radii (r_{ij}) [m]	0.43	0.43	0.43	0.47	0.47	0.47
Track width (w_{ij}) [m]	2.09	1.85	1.85	2.05	2.05	2.05
Longitudinal position relative CoG ($l_{a,ij}$) [m]	1.5344	1.8656	3.2356	1.2064	2.5064	3.8064

The distances from the CoG of each unit to the rear coupling point of the first unit d_{r_1} and to the front coupling point of the second unit d_{f_2} are set in meters as:

$$d_{r_1} = 2.1656 \tag{B.1}$$

$$d_{f_2} = 5.1936 \tag{B.2}$$

Other vehicle parameters necessary for complete simulations with VTM are omitted from this thesis due to confidentiality by Volvo GTT.

C

Results

Table C.1: Characteristic values of all vehicle setups for $\mu = 0.5$

Friction coefficient, μ	**Wheel angle, δ_{11}**	**Vehicle setup**	**Max yaw velocity [deg/s]**	**Responsiveness [m]**	**Final yaw angle [deg]**	**YSF, unit 1 For $t \in [1,2,3,4]$**				**YSF, unit 2 For $t \in [1,2,3,4]$**				**Max articulation angle [deg]**
0.5	9	1	18.46	3.15	-20.17	0.06	0.00	0.00	0.01	0.11	0.04	0.00	0.01	11.35
0.5	9.5	1	18.97	3.24	-24.63	0.28	0.01	0.01	0.01	0.39	0.03	0.00	0.01	11.84
0.5	10	1	19.43	3.32	-31.71	0.50	0.09	0.01	0.01	0.61	0.12	0.01	0.01	12.32
0.5	10.5	1	19.86	3.39	-73.68	0.68	0.67	0.65	0.55	0.64	0.61	0.68	0.67	12.81
0.5	11	1	20.24	3.46	-173.24	0.82	1.15	1.72	2.41	0.60	0.50	0.50	0.52	115.11
0.5	8	2	17.84	2.90	-19.18	0.03	0.00	0.00	0.01	0.04	0.04	0.00	0.01	11.12
0.5	8.5	2	18.50	3.02	-22.43	0.15	0.01	0.00	0.01	0.28	0.09	0.00	0.01	11.83
0.5	9	2	19.11	3.12	-28.17	0.42	0.01	0.00	0.01	0.72	0.20	0.02	0.01	12.58
0.5	9.5	2	19.70	3.21	-212.48	0.96	1.50	2.22	3.20	0.78	0.64	0.72	1.18	132.96
0.5	10	2	20.44	3.29	-270.38	1.33	2.03	3.02	4.73	0.60	0.43	0.51	0.09	219.77
0.5	8	3	17.84	2.96	-19.06	0.03	0.00	0.00	0.01	0.04	0.04	0.00	0.01	11.12
0.5	8.5	3	18.50	3.08	-22.31	0.15	0.01	0.00	0.01	0.28	0.09	0.00	0.01	11.83
0.5	9	3	19.11	3.18	-28.05	0.41	0.01	0.00	0.01	0.72	0.20	0.02	0.01	12.58
0.5	9.5	3	19.70	3.27	-219.61	0.95	1.46	2.28	3.38	0.67	0.33	0.44	0.60	163.84
0.5	10	3	20.30	3.35	-262.74	1.27	2.00	2.94	4.53	0.48	0.36	0.58	0.12	214.03
0.5	9	4	19.03	2.98	-31.69	0.29	0.05	0.03	0.03	0.43	0.05	0.03	0.03	12.71
0.5	9.5	4	19.52	3.06	-36.20	0.42	0.07	0.04	0.03	0.58	0.11	0.04	0.03	13.40
0.5	10	4	19.96	3.14	-44.13	0.60	0.23	0.04	0.04	0.68	0.36	0.07	0.04	14.07
0.5	10.5	4	20.35	3.21	-104.82	0.74	0.75	0.80	0.99	0.69	0.70	0.74	0.71	28.75
0.5	11	4	20.70	3.27	-197.93	0.86	1.25	1.87	2.68	0.65	0.58	0.55	0.56	131.18

Table C.2: Characteristic values of all vehicle setups for $\mu = 0.3$

Friction coefficient, μ	**Wheel angle, δ_{11}**	**Vehicle setup**	**Max yaw velocity [deg/s]**	**Responsiveness [m]**	**Final yaw angle [deg]**	**YSF, unit 1 For $t \in [1,2,3,4]$**				**YSF, unit 2 For $t \in [1,2,3,4]$**				**Max articulation angle [deg]**
0.3	10.5	1	14.09	2.40	-18.40	0.40	0.01	0.00	0.01	0.72	0.24	0.06	0.01	8.83
0.3	11	1	14.06	2.41	-16.55	0.31	0.01	0.00	0.01	0.60	0.26	0.03	0.01	8.75
0.3	11.5	1	14.01	2.42	-15.02	0.21	0.02	0.00	0.01	0.44	0.20	0.01	0.01	8.65
0.3	12	1	13.93	2.43	-13.69	0.13	0.01	0.00	0.01	0.28	0.14	0.00	0.01	8.53
0.3	12.5	1	13.83	2.44	-12.55	0.07	0.01	0.00	0.00	0.14	0.10	0.00	0.01	8.41
0.3	5.5	2	11.78	1.94	-16.06	0.33	0.01	0.00	0.01	0.60	0.18	0.01	0.01	7.65
0.3	6	2	12.36	2.03	-23.18	0.62	0.19	0.02	0.00	0.88	0.35	0.24	0.01	8.28
0.3	6.5	2	12.82	2.11	-57.09	0.77	0.74	0.75	0.78	0.85	0.84	0.86	0.97	8.77
0.3	7	2	13.39	2.17	-124.26	0.91	1.26	1.90	2.68	0.72	0.34	0.20	0.42	92.00
0.3	7.5	2	13.84	2.22	-143.00	1.00	1.47	2.14	3.01	0.60	0.18	0.31	0.47	111.86
0.3	5.5	3	11.75	1.96	-15.33	0.28	0.02	0.00	0.01	0.51	0.16	0.01	0.01	7.58
0.3	6	3	12.34	2.05	-20.13	0.53	0.03	0.00	0.01	0.85	0.07	0.10	0.01	8.16
0.3	6.5	3	12.85	2.13	-27.86	0.67	0.45	0.02	0.00	0.87	0.80	0.23	0.15	8.62
0.3	7	3	13.36	2.19	-93.09	0.78	0.94	1.33	1.87	0.77	0.54	0.18	0.35	58.04
0.3	7.5	3	13.82	2.24	-121.89	0.92	1.26	1.76	2.49	0.61	0.25	0.32	0.40	90.21
0.3	10.5	4	13.29	2.27	-18.04	0.23	0.02	0.00	0.01	0.46	0.09	0.00	0.01	8.92
0.3	11	4	12.85	2.29	-14.89	0.06	0.00	0.00	0.01	0.15	0.04	0.00	0.01	8.34
0.3	11.5	4	12.35	2.29	-12.82	0.01	0.00	0.00	0.01	0.03	0.02	0.00	0.01	7.81
0.3	12	4	14.24	2.32	-15.03	0.13	0.01	0.00	0.00	0.27	0.07	0.01	0.00	9.11
0.3	12.5	4	14.09	2.31	-13.52	0.05	0.00	0.00	0.00	0.11	0.04	0.00	0.00	8.86

DEPARTMENT OF MECHANICS OF MARITIME SCIENCES
CHALMERS UNIVERSITY OF TECHNOLOGY
Gothenburg, Sweden
www.chalmers.se

CHALMERS
UNIVERSITY OF TECHNOLOGY